

1 **Analogue experiments on releasing and restraining bends and their**
2 **application to the study of the Barents Shear Margin**

3
4
5
6 **Roy H. Gabrielsen¹⁾, Panagiotis A. Giannenas²⁾, Dimitrios Sokoutis^{1,3)}, Ernst**
7 **Willingshofer³⁾, Muhammad Hassaan^{1,4)} & Jan Inge Faleide¹⁾**

8
9 ¹⁾ Department of Geosciences, University of Oslo, Norway

10 ²⁾ Univ Rennes, CNRS, Géosciences Rennes, UMR 6118, 35000 Rennes, France

11 ³⁾ Faculty of Geosciences, Utrecht University, the Netherlands

12 ⁴⁾ Vår Energi AS, Grundingen 3, 0250 Oslo, Norway

13
14
15 **Corresponding author: Roy H. Gabrielsen (r.h.gabrielsen@geo.uio.no)**

16
17 **ORCI-id:**

18 Jan Inge Faleide: 0000-0001-8032-2015

19 Roy H. Gabrielsen: 0000-0001-5427-8404

20 Muhammad Hassaan: 0000-0001-6004-8557

21
22
23
24
25 **Abstract:**

26 The Barents Shear Margin separates the Svalbard and Barents Sea from the
27 North Atlantic. During the break-up of the North Atlantic the plate tectonic
28 configuration was characterised by sequential dextral shear, extension, and
29 eventually contraction and inversion. This generated a complex zone of
30 deformation that contains several structural families of over-lapping and
31 reactivated structures.

32 A series of crustal-scale analogue experiments, utilising a scaled stratified sand-
33 silicon polymer sequence were utilised in the study of the structural evolution of
34 the shear margin.

35
36 The most significant observations for interpreting the structural configuration of
37 the Barents Shear Margin are:

38 1) Prominent early-stage positive structural elements (e.g. folds, push-ups)
39 interacted with younger (e.g. inversion) structures and contributed to a hybrid
40 final structural pattern.

41 2) Several structural features that were initiated during the early (dextral shear)
42 stage became overprinted and obliterated in the subsequent stages.

43 3) All master faults, pull-part basins and extensional shear duplexes initiated
44 during the shear stage quickly became linked in the extension stage, generating a
45 connected basin system along the entire shear margin at the stage of maximum
46 extension.

47 4) The fold pattern generated during the terminal stage (contraction/inversion
48 became dominant in the basin areas and was characterised by fold axes striking
49 parallel to the basin margins. These folds, however, strongly affected the shallow
50 intra-basin layers.

51 The experiments reproduced the geometry and positions of the major basins and
52 relations between structural elements (fault and fold systems) as observed along
53 and adjacent to the Barents Shear Margin. This supports the present structural
54 model for the shear margin.

55
56

57 **Plain language summary:**

58 The Barents Shear Margin defines the border between the relatively shallow
59 Barents Sea that is situated on a continental plate, and the deep ocean. The
60 margin is characterised by a complex structural pattern that has resulted from
61 the opening and separation of the continent and the ocean, starting c. 65 million
62 years ago. This history included on phase of right-lateral shear and one phase of
63 spreading, the latter including a sub-phase of shortening, perhaps due to plate
64 tectonic reorganizations. The area has been mapped by the study of reflection
65 seismic lines for decades, but many details of its development is not yet fully
66 constrained. We therefore ran a set of scaled experiments to investigate what
67 kind of structures could be expected in tectonic environment, and to figure out
68 what is a reasonable time relation between them. From these experiments we
69 deduced several types of structures (faults, folds and sedimentary basins) that
70 help us to improve the understanding of the history of the opening of the North
71 Atlantic.

72
73
74

75 **Key words:** Analogue experiments, dextral strike-slip, releasing and restraining
76 bends, multiple folding, Barents Shear Margin, basin inversion

77
78

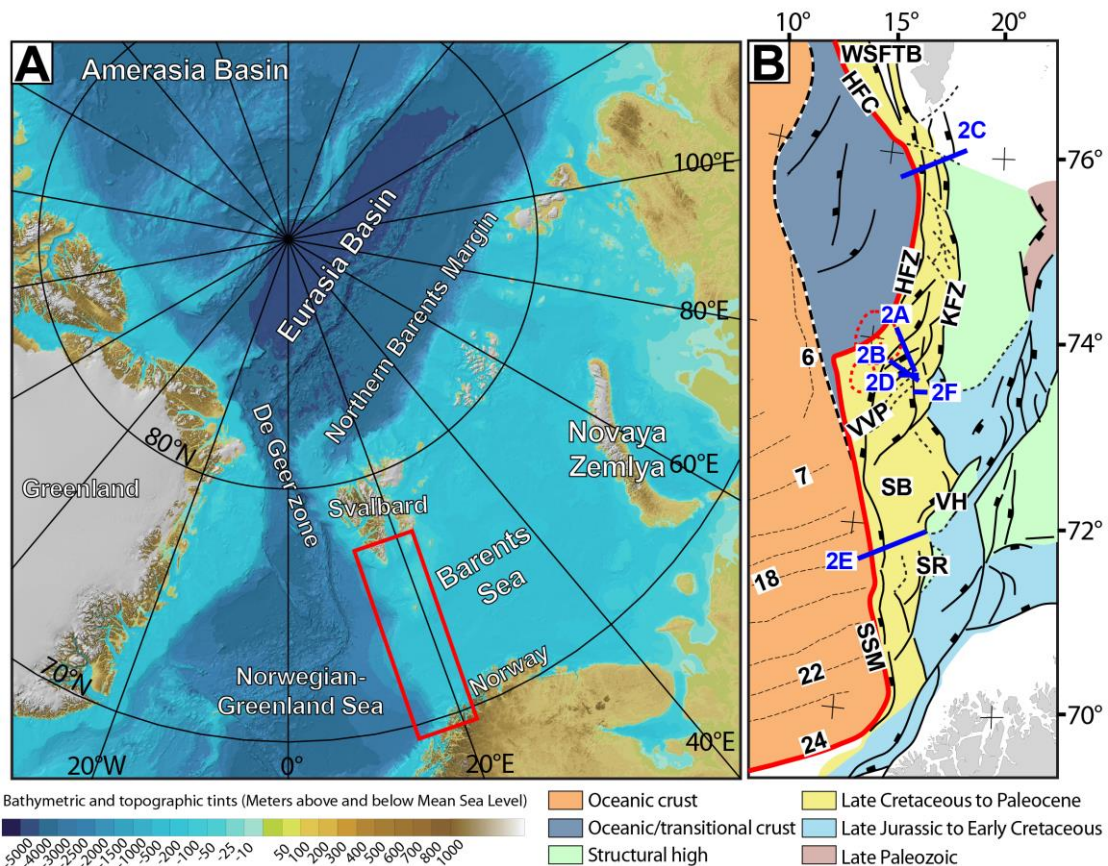
79 **Introduction**

80

81 Physiography, width and structural style of the Norwegian continental margin
82 vary considerably along its strike (e.g. Faleide et al., 2008, 2015). The margin
83 includes a southern rifted segment between 60° and 70°N and a northern
84 sheared-rifted segment between 70° and 82°N (**Figure 1A**). The latter coincides
85 with the ocean-ward border of the western Barents Sea and Svalbard margins
86 (e.g. Faleide et al., 2008) and is referred to here as “the Barents Shear Margin”.
87 This segment coincides with the continent-ocean transition (COT) of the
88 northernmost part of the North Atlantic Ocean. Its configuration is typical for
89 that of transform margins where the structural pattern became established in an
90 early stage of shear, later to develop into an active continent-ocean passive
91 margin (Masclé & Blarez, 1987; Lorenzo, 1997; Seiler et al., 2010; Basile, 2015;
92 Nemcok et al., 2016).

93 Late Cretaceous - Palaeocene shear, rifting, breakup and incipient spreading in
94 the North Atlantic was associated with voluminous magmatic activity, resulting
95 in the development of the North Atlantic Volcanic Province (Saunders et al.,
96 1997; Ganerød et al., 2010; Horni, 2017). According to its tectonic development,
97 the Barents Shear Margin (**Figure 1B**) incorporates, or is bordered by, several
98 distinct structural elements, some of which are associated with volcanism and
99 halokinesis.

100 The multistage development combined with a complex geometry caused
101 interference between structures (and sediment systems) in different stages of
102 the margin development. Such relations are not always obvious, but
103 interpretation can be supported by the help of scale-models. We combine the
104 interpretation of reflection seismic data and analogue modeling. Thus, we
105 investigate structures generated in dextral shear. These were generated during
106 initial dextral shear the development into seafloor spreading and subsequent
107 contraction. The later stages (contraction) were likely influenced by plate
108 reorganization (Talwani & Eldholm, 1977; Gaina et al., 2009; see also Våagnes et
109 al., 1998; Pascal & Gabrielsen, 2001; Pascal et al., 2005; Gac et al., 2016) or other
110 far-field stresses (Doré & Lundin, 1996; Lundin & Doré, 1997; Doré et al., 1999;
111 2016; Lundin et al., 2013). The present experiments were designed to illuminate
112 the structural complexity affiliated with multistage sheared passive margins, so



113

114 **Figure 1: A)** The Barents Sea is separated from the Norwegian-Greenland Sea by
 115 the de Geer transfer margin. Red box shows the present study area. **B)** Structural
 116 map of the Barents Sea Shear Margin. Note segmentation of the continent-ocean
 117 transition. Abbreviations (from north to south): WSFTB = West Spitsbergen
 118 Fold-and-Thrust Belt, HFZ = Hornsund Fault Complex, KFC = Knølegga Fault
 119 Zone, VVP = Vestbakken Volcanic Province, SB = Sørvestsnaget Basin, VH =
 120 Veslemøy High, SR = Senja Ridge, SSM = Senja Shear Margin. Blue lines indicate
 121 position of seismic profiles in Figure 2 and red line X-X' shows western border of
 122 thinned crust (see also Figure 3). Chron numbers are indicated on oceanic crust
 123 area.

124

125 that the significance of structural elements like fault and fold systems observed
 126 along the Barents Shear Margin could be set into a dynamic context. The study
 127 area suffered repeated and contrasting stages of deformation, including dextral
 128 shear, oblique extension, inversion and volcanic activity. This is a particular
 129 challenge in such tectonic settings that are characterised by repeated
 130 overprinting and cannibalization of younger structural elements. Results from
 131 the the experiments facilitate the identification and characterization of structural
 132 elements at the different stages of deformation. Additionally, they allow to

133 identify the structural elements that were developed at stages of deformation
134 preceding the present-day margin configuration.

135

136 **Regional background**

137 In the following sections we provide definitions and a short description of the
138 main structural elements constituting the study area. The structural elements
139 are presented in-sequence from north to south (**Figure 1B**).

140 The greater **Barents Shear Margin** is a part of the more extensive De
141 Geer Zone mega shear system which linked the Norwegian Greenland Sea and
142 the Arctic Eurasia system (Eldholm et al., 1987; 2002; Faleide et al., 1988;
143 Breivik et al., 1998; 2003). Together with its conjugate Greenland counterpart it
144 carries the evidence of post-Caledonian extension that culminated with Cenozoic
145 break-up of the North Atlantic (e.g. Brekke, 2000; Gabrielsen et al., 1990; Faleide
146 et al., 1993; Gudlaugsson et al., 1998). Two shear margin segments are separated
147 by a central rift-dominated segment along the Barents Shear Margin (Myhre et
148 al., 1982; Vågnes, 1997; Myhre & Eldholm, 1988; Ryseth et al., 2003; Faleide et
149 al., 1988; 1993; 2008). Each segment maintained the structural and magmatic
150 characteristics of the crust during its development. Of these the Senja Shear
151 Margin is the southernmost segment, originally termed the Senja Fracture Zone
152 by Eldholm et al. (1987). Here NNW-SSE-striking folds interfere with NE-SW-
153 striking structures (Giannenas, 2018). Strain partitioning characterizes the shear
154 zone system (e.g. West Spitsbergen; Leever et al., 2011a,b and the Sørvestsnaget
155 Basin; Kristensen et al., 2017).

156

157 **The Hornsund Fault Zone and West Spitsbergen Fold-and Thrust Belt** form
158 the northernmost segment of the Barents Shear Margin. It coincides with the
159 southern continuation of the De Geer Zone and the Senja Shear Margin. The
160 Hornsund Fault Zone belongs to this system and provides a type setting for
161 transpression and strain partitioning together with the West Spitsbergen fold-
162 and-thrust-belt (Harland, 1965; 1969; 1971; Lowell, 1972; Gabrielsen et al.,
163 1992; Maher et al., 1997; Leever et al., 2011 a,b). Plate tectonic reconstructions
164 suggest that the plate boundary accommodated c. 750 km along-strike dextral

165 displacement and 20-40 km of shortening in the Eocene (Bergh et al., 1997;
166 Gaina et al., 2009).

167

168 **The Knølegga Fault Zone** can be seen as a part of the Hornsund fault system
169 extending from the southern tip of Spitsbergen (Gabrielsen et al., 1990). It trends
170 NNE-SSW to N-S and defines the western margin of the Stappen High. The
171 vertical displacement approaches 6 km. Although the main movements along the
172 fault may be Tertiary of age, it is likely that it was initiated much earlier. The
173 Tertiary displacement may have a lateral (dextral) component (Gabrielsen et al.,
174 1990).

175

176 **The Vestbakken Volcanic Province** is the main topic of this contribution. It
177 represents the central rifted segment of the Barents Shear Margin and links the
178 sheared margin segments to the north and south occupying a right-double
179 stepping (eastward) releasing-bend-setting. Prominent volcanoes and sill-
180 intrusions suggest three distinct volcanic events in the Vestbakken Volcanic
181 Province (Jebsen & Faleide, 1998; Faleide et al., 2008; Libak et al., 2012). It is
182 constrained to its east by the eastern boundary fault (EBF in **Figure 1B**), that is a
183 part of the Knølegga Fault Complex, separating the Vestbakken Volcanic Province
184 from the marginal Stappen High to the east. To the south and southeast the
185 Vestbakken Volcanic Province drops gradually towards the Sørvestsnaget Basin
186 across the southern extension of the eastern boundary fault and its associated
187 faults. To the west and north the area is delineated by the continent – ocean
188 boundary/transition. The Vestbakken Volcanic Province includes both
189 extensional and contractional structures (e.g. Jebsen & Faleide, 1998; Faleide et
190 al., 2008; Blaich et al., 2017). Two main episodes of Cenozoic extensional faulting
191 were identified in the Vestbakken Volcanic Province: (i) a late Paleocene-early
192 Eocene event, which correlates in time with the continental break-up in the
193 Norwegian-Greenland Sea, (ii) an early Oligocene event that is tentatively
194 correlated to plate reorganization around 34 Ma activating NE-SW striking faults.
195 Volcanic activity coincides with these events.

196

197 **The Sørvestsnaget Basin** occupies the area east of the COT between 71 and
198 73°N and is characterised by an exceptionally thick Cretaceous-Cenozoic
199 sequence (Gabrielsen et al., 1990). To the west it is delineated by the Senja Shear
200 Margin and to the northeast it is separated from the Bjørnøya Basin by the
201 southern part of the Knølegga Fault Complex (Faleide et al., 1988). The position
202 of the Senja Ridge coincides with southeastern border of the Sørvestsnaget Basin
203 (**Figure 1B**), whereas the Vestbakken Volcanic Province is situated to its north.
204 An episode of Cretaceous rifting in the Sørvestsnaget Basin climaxed in the
205 Cenomanian-middle Turonian (Breivik et al., 1998), succeeded by Late
206 Cretaceous-Palaeocene fast sedimentation (Ryseth et al., 2003). Particularly the
207 later stages of the basin formation were strongly influenced by the opening of
208 the North Atlantic (Hanisch, 1984; Brekke & Riis, 1987). Salt diapirism also
209 contributed to the development of this basin (Perez-Garcia et al., 2013).

210

211 **The Senja Ridge** (SR in **Figure 1B**) runs parallel to the continental margin and
212 coincides with the western border of the Tromsø Basin. It is characterised by a
213 N-S-trending gravity anomaly which is interpreted as buried mafic-ultramafic
214 intrusions which are associated with the Seiland Igneous Province (Fichler &
215 Pastore, 2022). The structural development of the Senja Ridge has been
216 associated with shear affiliated with the development of the shear margin (Riis
217 et al., 1986) and though it documented that it was a positive structural element
218 from the mid Cretaceous to the Pliocene it may have been activated at an even
219 earlier stage (Gabrielsen et al., 1990).

220

221 **The Senja Shear Margin** was active during the Eocene opening of the
222 Norwegian-Greenland Sea dextral shear causing splitting off of slivers of
223 continental crust. These slivers became embedded in the oceanic crust during
224 continued seafloor spreading (Faleide et al., 2008). The Senja Shear Margin
225 coincides with the western margin of a basin system superimposed on an area of
226 significant crustal thinning. This part of the shear margin was characterised by a
227 composite architecture even during the earliest stages of its development
228 (Faleide et al., 2008). The basin system accumulated sedimentary sequences that
229 reached thicknesses of up to 18-20 km. Subsequent shearing contributed to the

230 development of releasing and restraining bends, associated pull-apart-basins,
231 neutral strike-slip segments, flower-structures and fold-systems (*sensu* Crowell,
232 1974 a,b; Biddle & Christie-Blick, 1985a,b; Cunningham & Mann, 2007a,b).
233 Particularly the hanging wall west of the Knølegga Fault Complex (see below) of
234 the Barents Shear Margin was affected by wrench deformation as seen from
235 several push-ups and fold systems (Grogan et al., 1999; Bergh & Grogan 2003).
236 The structural development of the margin was complicated by active halokinesis
237 (Knutsen & Larsen, 1997; Gudlaugsson et al., 1998; Ryseth et al., 2003).

238

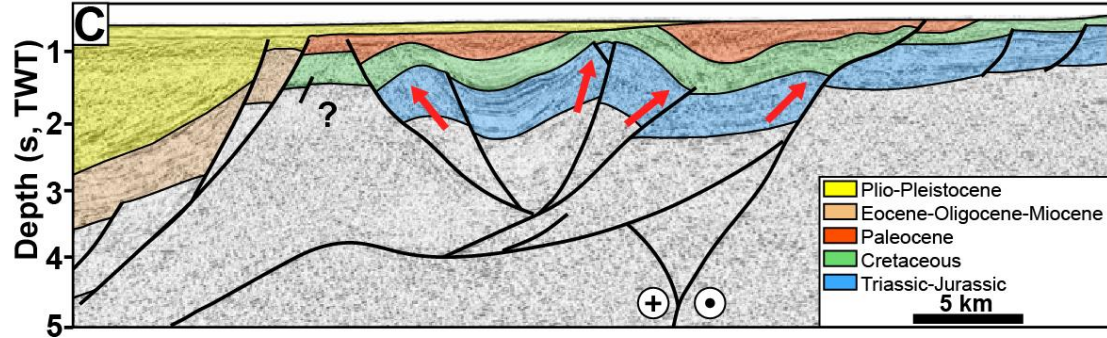
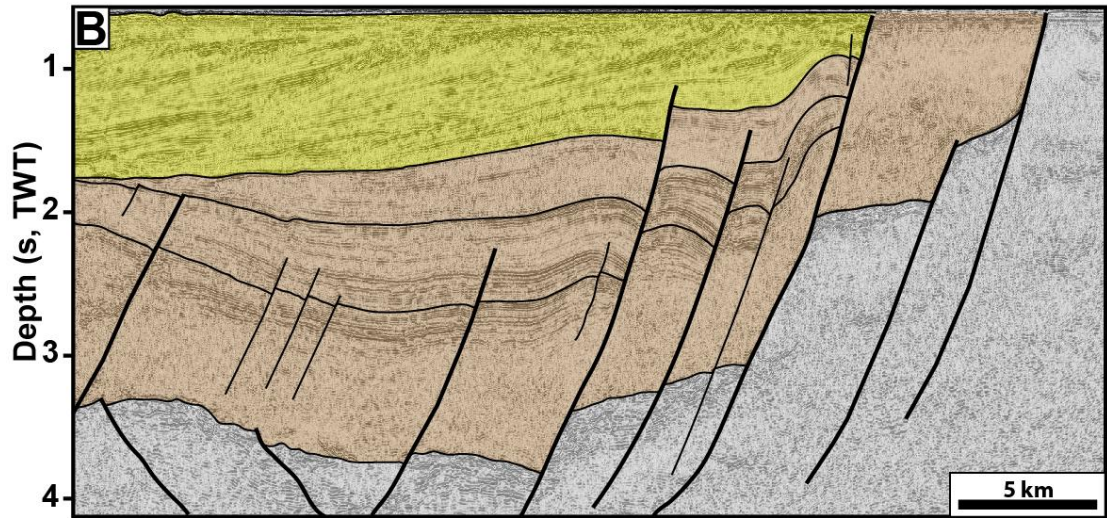
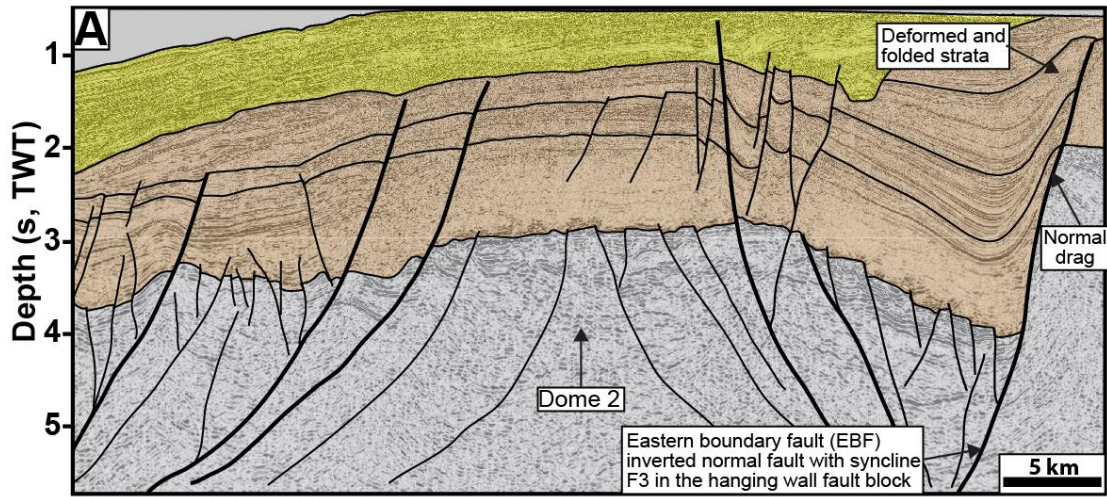
239 **Reflection seismic data and structural interpretation**

240 The data set of this study includes 2D seismic reflection data from several surveys
241 and well data in the Vestbakken Volcanic Province. Data coverage is less dense in the
242 northern part of the study area. Typical spacing of seismic lines is 4 km. Well 7316/5-
243 1 was used to correlate the seismic data with formation tops in the study area while
244 previously published correlations provided calibration and age of each seismic
245 horizon (e.g. Eidvin et al., 1993; 1998 Ryseth et al., 2003). Three stratigraphic groups
246 are encountered in the well, namely the Nordland Group (between 473 - 945 m); the
247 Sotbakken Group (between 945-3752m) and Nygrunnen Group (between 3752-
248 4014m) (Eidvin et al., 1993; 1998; www.npd.no). Several folds of regional
249 significance and with axial traces that can be followed along strike for 2-3 km or more
250 occur in the Vestbakken Volcanic Province. The folds are commonly situated in the
251 hanging walls of extensional faults and the fold traces and the structural grain of the
252 thick-skinned master faults are generally parallel. This shows that the position and
253 orientation of the folds were determined by the preexisting basement structural fabric.
254 The mapping of the folds is constrained by the spacing of reflection seismic lines, so
255 each fold trace may include undetected overlap-zones or axial off-sets. The folds were
256 identified on the lower Eocene, Oligocene and lower Miocene levels. All the mapped
257 folds are either positioned in the hanging walls of extensional (sometimes inverted)
258 master faults or are dissected by younger faults with minor throws.

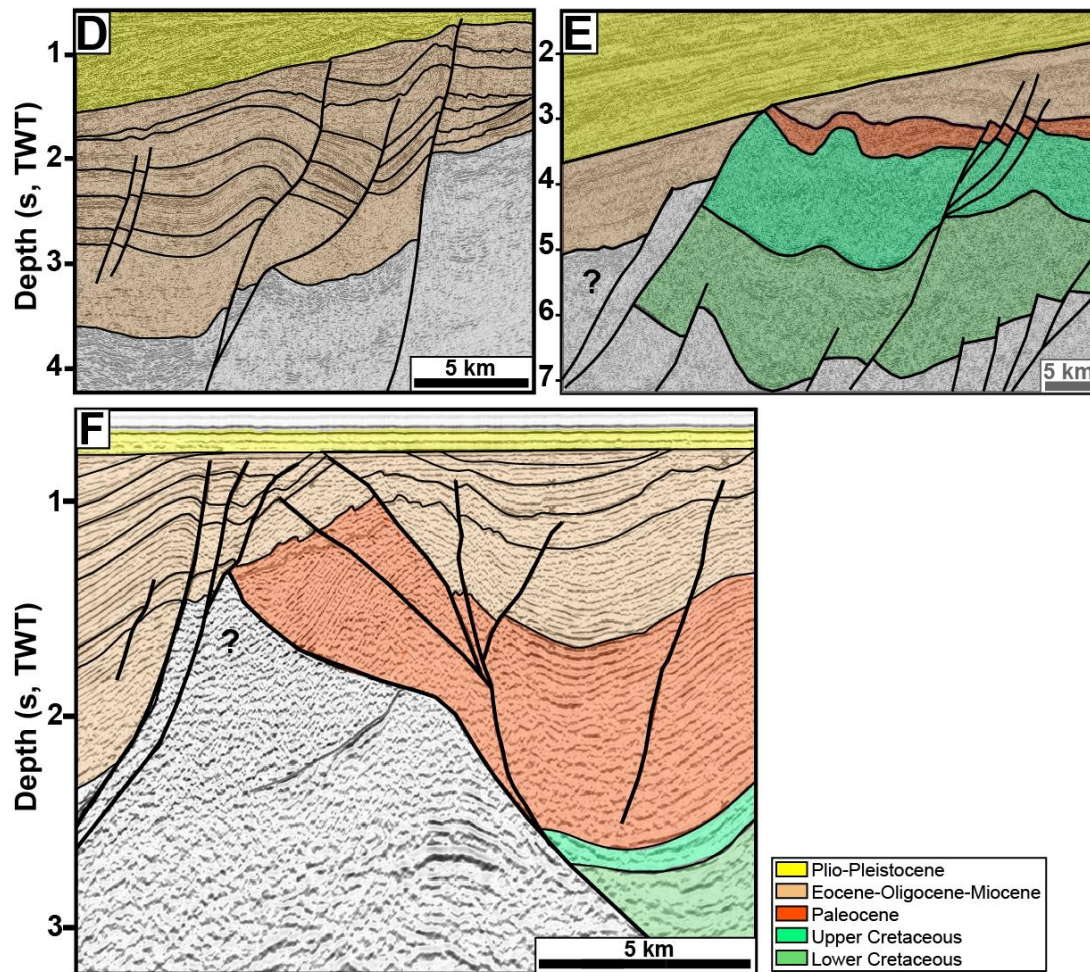
259

260 **Strike-slip systems and analogue shear experiments**

261 Shear margins and strike-slip systems are structurally complex and highly
262 dynamic, so that the ultimate architecture of such systems contains structural



263
 264
 265
 266
 267
 268
 269
 270
 271



272

273 **Figure 2:** Seismic examples, Vestbakken Volcanic Province. **A)** Gentle, partly
 274 collapsed NE-SW-striking anticline/dome of uncertain origin in the eastern
 275 terrace domain of the southern Vestbakken Volcanic Province. **B,C)**
 276 Asymmetrical folds (fold family 2; Giannenas 2018) situated along the eastern
 277 margin of the Vestbakken Volcanic Province. These may represent primary SPE-
 278 4-structures focused in the hanging walls along margins of master fault blocks,
 279 representing reactivated SPE-2-structures. **D)** trains of symmetrical folds with
 280 upright fold axes (corresponding to PSE-5-structures) are preserved inside
 281 larger fault blocks. See text for explanation of SPE-structures. **E)** Section through
 282 push-up associated with restraining bend (PSE-4-structure). **F)** Flower (PSE-2)-
 283 structure in area dominated by neutral shear.

284

285 elements that were not contemporaneous (e.g. Graymer et al., 2007; Crowell,
 286 1962; 1974a,b; Woodcock & Fischer, 1986; Mousloupoulou et al., 2007; 2008).
 287 Analogue models offer the option to study the dynamics of such relations and
 288 therefore attracted the attention of early workers in this field (e.g. Cloos, 1928;
 289 Riedel, 1929) and have continued to do so until today. Early experimental works
 290 mostly utilised one-layer (“Riedel-box”) models (e.g. Emmons, 1969; Tchalenko,
 291 1970; Wilcox et al., 1973), which were soon to be expanded by the study of

292 multilayer systems (e.g. Faugère et al., 1986; Naylor et al., 1986; Richard et al.,
293 1991; Richard & Cobbold, 1989, 1995; Schreurs, 1994, 2003; Manduit & Dauteuil,
294 1996; Dateuil & Mart, 1998; Schreurs & Colletta, 1998, 2003; Ueta et al., 2000;
295 Dooley & Schreurs, 2012). The systematics and dynamics of strike-slip systems
296 have been focused upon in a number of summaries like Sylvester (1985; 1988);
297 Biddle & Christie-Blick (1985 a,b); Cunningham & Mann (2007); Dooley &
298 Schreurs (2012); Nemcok et al. (2016) and Peacock et al. (2016). Concepts and
299 nomenclature established in these works are used in the following descriptions
300 and analysis. Also, following Christie-Blick & Biddle (1985a,b) and Dooley &
301 Schreurs (2012) we apply the term Principal Deformation Zone (PDZ) for the
302 junction between the movable polythene plates underlying the experiment. The
303 contact between the fixed and movable base defined a non-stationary velocity
304 discontinuity (“VD”; Ballard et al., 1987; Allemand & Brun, 1991; Tron & Brun,
305 1991).

306 Several experimental works have particularly focused on the geometry
307 and development of pull-apart-basins in releasing bend settings (Mann et al.,
308 1983; Faugère et al., 1983; Richard et al., 1995; Dooley & McClay, 1997; Basile &
309 Brun, 1999; Sims et al., 1999; Le Calvez & Vendeville, 2002; Mann, 2007; Mitra &
310 Paul, 2011). The pull-apart basin was described by Burchfiel & Stewart (1966)
311 and Crowell (1974a,b) as formed at a releasing bend or at a releasing fault step-
312 over along a strike-slip zone (Biddle & Christie-Blick, 1985a,b). This basin type
313 has also been termed “rhomb grabens” (Freund, 1971) and “strike-slip basins”
314 (Mann et al., 1993) and is commonly considered to be synonymous with the
315 extensional strike-slip duplex (Woodcock & Fischer, 1986; Dooley & Schreurs,
316 2012). In the descriptions of our experiments, we found it convenient to
317 distinguish between extensional strike-slip duplexes in the context of Woodcock
318 & Fischer (1986) and Twiss & Moores (2007, p. 140-141) and pull-apart basins
319 (rhomb grabens: Crowell, 1974 a,b; Aydin & Nur, 1993) since they reflect slightly
320 different stages in the development in our experiments (see discussion).

321

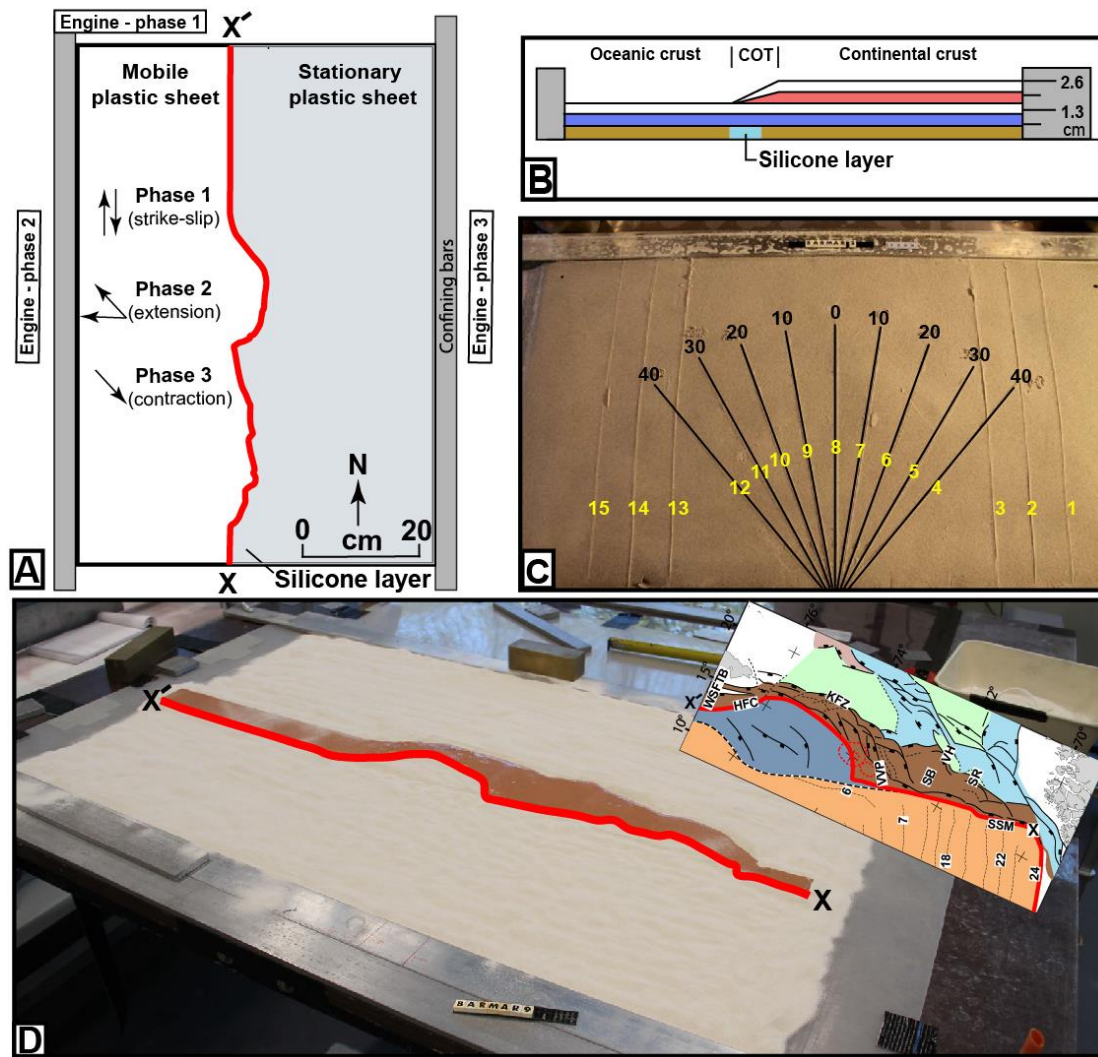
322 **Experimental setup**

323 To study the kinematics of complex shear margins, a series of analogue
324 experiments were performed at the tectonic modelling laboratory (TecLab) of

325 Utrecht University, The Netherlands. All experiments were built on two
326 overlapping 1 mm thick plastic sheets (each 100 cm long and 50 cm wide) that
327 were placed on a flat, horizontal table surface. The boundary between the
328 underlying movable and overlying stationary plastic sheets had the shape of the
329 mapped continent-ocean boundary (COB; **Figure 1B**). The moveable sheet was
330 connected to an electronic engine, which pulled the sheet at constant velocity
331 during all three deformation stages. Displacement rates were therefore not
332 scaled. The modelling material was then placed on these sheets where the layers
333 on the stationary sheet represent the continental crust including the continent-
334 ocean transition (COT) whereas those on the mobile sheet represent the oceanic
335 crust. The model layers were confined by aluminum bars along the long sides
336 and sand along the short sides (**Figure 3A**). The continental crust tapers off
337 towards the oceanic crust with a relatively constant gradient. A sand-wedge with
338 a constant dip angle determined by the difference in thickness between the
339 intact and the stretched crust, and that covered the width of the silicon putty
340 layer, was made to simulate the ocean-continent transition (**Figure 3B**). The
341 taper angle was kept constant for all models.

342 The pre-cut shape of the plate boundary includes major releasing bends
343 positioned so that they correspond to the geometry of the COB and the three
344 main structural segments of the Barents Shear Margin as follows. *Segment 1* of
345 the BarMar-experiments (**Figure 4**) contained several sub-segments with
346 releasing and restraining bends as well as segments of “neutral” (Wilcox et al.,
347 1973; Mann et al. 1983; Biddle & Christie-Blick, 1985b) or “pure” (Richard et al.,
348 1991) strike-slip. *Segment 2* had a basic crescent shape, thereby defining a
349 releasing bend at its southern margin in the position similar to that of the
350 Vestbakken Volcanic Province that merged into a neutral shear-segment along
351 the strike of, whereas a restraining bend occupied the northern margin of the
352 segment. *Segment 3* was a straight basement segment, defining a zone of neutral
353 shear and corresponds to the strike-slip segment west of Svalbard (**Figure 1**).

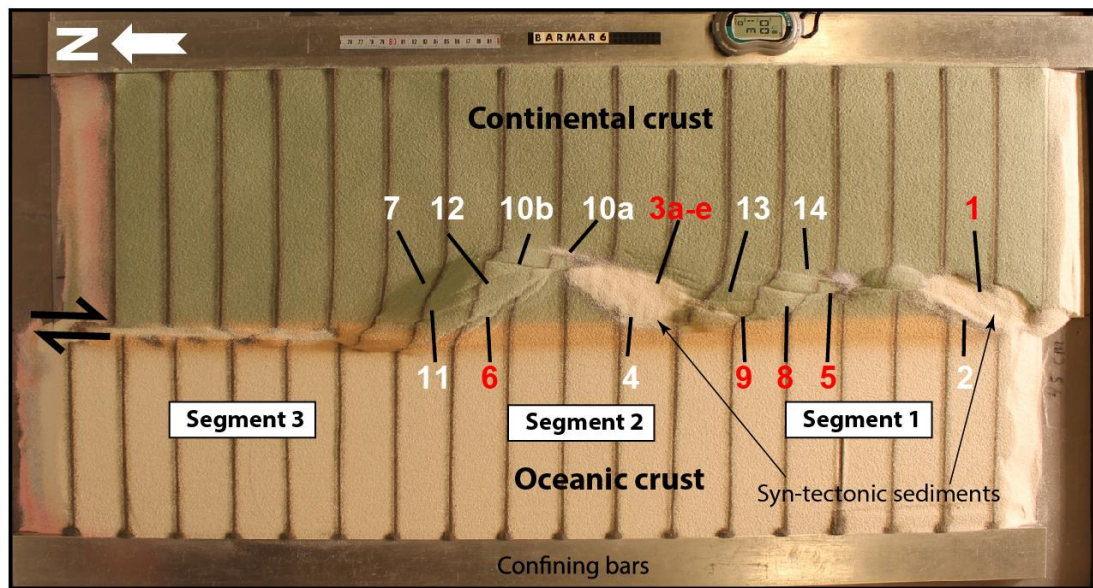
354 The experiments included three stages of deformation with constant rates
355 of movement of the mobile sheet at 10 cmhr⁻¹ in all three stages. The relative
356 angles of plate movements in the experiments were taken from post late
357 Paleocene opening directions in the northeast Atlantic (Gaina et al., 2009).



358

359 **Figure 3: A)** Schematical set-up of BarMar3-experiment as seen in map view. **B)**
 360 Section through same experiment before deformation, indicating stratification
 361 and thickness relations. **C)** Standard positions and orientation for sections cut in
 362 all experiments in the BarMar-series. Yellow numbers are section numbers.
 363 Black numbers indicate angle between the margins of the experiment (relative to
 364 N-S) for each profile. **D)** Outline of silicone putty layer as applied in all
 365 experiments. Inset shows original structural map of the Barents Margin used to
 366 define the width of the thinned crust. Red line (X-X') indicates the western limit
 367 of the thinned zone.
 368

369 Dextral shear was applied in the *first phase* in all experiments by pulling the
 370 lower plastic sheet by 5 cm. In the *second phase* the left side of the experiment
 371 was extended by 3 cm orthogonally (BarMar6) or obliquely (315 degrees;
 372 BarMar 8 & 9) to the trend of the shear margin, whereas plate motion was
 373 reversed during the *third phase of deformation*, leading to inversion of earlier
 374 formed basins that had been developed in the strike-slip and extensional phases.
 375 Sedimentary basins that develop due to strike-slip (phase 1) or extension (phase



376

377 **Figure 4:** Position of segments and major structural elements as referred to in
 378 the text and subsequent figures (see particularly **Figures 5 and 6**). This example
 379 is taken from the reference experiment BarMar6. All experiments BarMar6-9
 380 followed the same pattern, and the same nomenclature was used in the
 381 description of all experiments and provides the template for the definition of
 382 structural elements in **Figure 7**.

383

384 2) have been filled with layers of colored feldspar sand by sieving, so that a
 385 smooth surface was obtained. These layers are primarily important for
 386 discriminating among deformation phases and thus act as marker horizons.
 387 Phase 3 was initiated by inverting the orthogonal (BarMar6) or oblique (BarMar
 388 8 & 9) extension of Phase 2 to contraction as a proxy for ridge-push that likely
 389 was initiated when the mid-oceanic ridge was established in Miocene time in the
 390 North Atlantic (Moser et al., 2002; Gaina et al., 2009). Contraction generated by
 391 ridge-push has been inferred from the mid Norwegian continental shelf (Våagnes
 392 et al., 1998; Pascal & Gabrielsen, 2001; Faleide et al., 2008; Gac et al., 2016) and
 393 seems still to prevail in the northern areas of Scandinavia (Pascal et al., 2005),
 394 although far-field compression generated by other processes have been
 395 suggested (e.g. Doré & Lundin, 1996).

396 Coloured layers of dry feldspar sand represent the brittle oceanic and
 397 continental crust. This material has proven suitable for simulating brittle
 398 deformation conditions (Willingshofer et al., 2005; Luth et al., 2010; Auzemery et
 399 al., 2021). It is characterised by a grain size of 100-200 μm , a density of 1300
 400 kgm^{-3} , a cohesion of $\sim 16\text{-}45$ Pa and a peak friction coefficient of 0.67

401 (Willingshofer et al., 2018). Additionally, a 8 mm thick and of variable width
402 corresponding to the transition zone (as mapped in reflection seismic data) of
403 'Rhodorsil Gomme GSIR' (Sokoutis, 1987) silicone putty mixed with fillers was
404 used as a proxy for the thinned and weakened continental crust at the ocean-
405 continent transition (**Figure 1B and 3A,B**). This Newtonian material ($n=1.09$)
406 has a density of 1330 kgm^{-3} and a viscosity of $1.42 \times 10^4 \text{ Pa.s}$.

407 The experiments were scaled following standard scaling procedures as
408 described by Hubbert (1937), Ramberg (1967) or Weijermars and Schmeling
409 (1986), assuming that inertia forces are negligible when modelling tectonic
410 processes on geologic timescales (see Ramberg (1981) and Del Ventisette et al.
411 (2007) for a discussion on this topic). The models were scaled so that 10 mm in
412 the model approximates c. 10 km in nature yielding a length scale ratio of 1.00×10^{-6} .
413 As such, the model oceanic and continental crusts scale to 18 and 26 km in
414 nature, respectively, which, although slightly overestimating the oceanic crustal
415 thickness (10-12 km) is in full agreement with the estimated thickness of the
416 thinned oceanward segment of the continental crust (30-20 km; Breivik et al.,
417 1998).

418 The brittle crust, dry feldspar sand, deforms according to the Mohr-
419 Coulomb fracture criterion (Horsfield, 1977; Mandl et al., 1977; McClay, 1990;
420 Richard et al., 1991; Klinkmüller et al., 2016), whereas silicone putty promotes
421 ductile deformation and folding. The configuration applied in the present
422 experiments is accordingly well suited for the study of the COB in the Barents
423 Shear Margin (Breivik et al., 1998).

424 When complete, the experiments were covered with a thin layer of sand
425 further to stabilize the surface topography before the models were saturated
426 with water and cross-sections that were oriented transverse to the velocity
427 discontinuity were cut in a fan-shaped pattern (**Figure 3C**). All experiments have
428 been monitored with a digital camera providing top-view images at regular time
429 intervals of one minute.

430 All experiments performed were oriented in a N-S-coordinate framework
431 to facilitate comparison with the western Barents Sea area and had a three-stage
432 deformation sequence (dextral shear – extension – contraction). All descriptions
433 and figures relate to this orientation. It was noted that all experiments

434 reproduced comparable basic geometries and structural types, demonstrating
435 robustness against variations in contrasting strength of the “ocean-continent”-
436 transition zone, which included a zone of silicone putty with variable width
437 below an eastward thickening sand-wedge (**Figure 3B**). The experiments were
438 terminated before the full closure of the basin system, in accordance with the
439 extension vector > contraction vector as in the North Atlantic (see Vågnes et al.
440 1998; Pascal & Gabrielsen 2001; Gaina et al. 2009).

441

442 **Modelling Results**

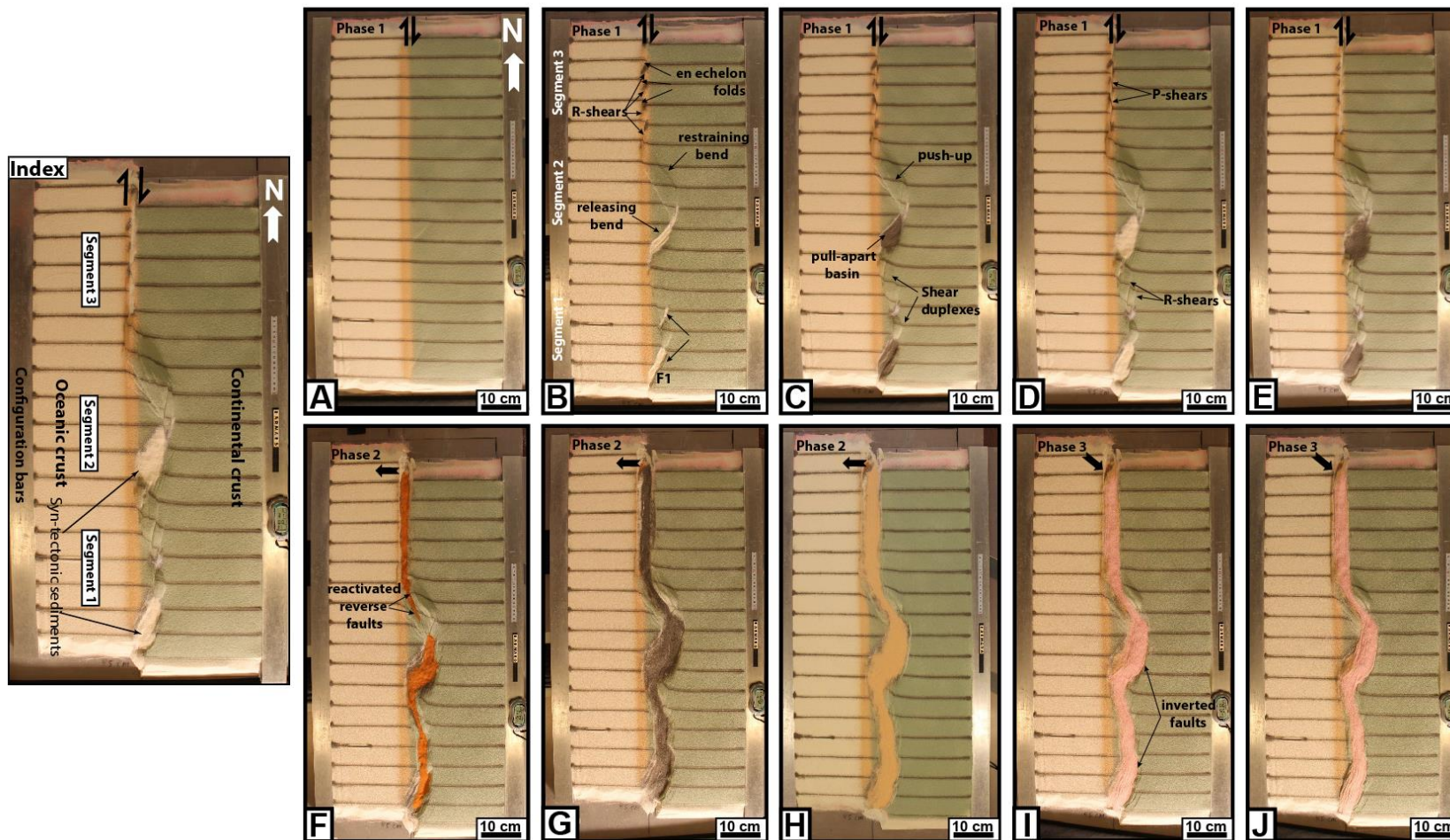
443 A series of nine experiments (BarMar1-9) with the set-up described above was
444 performed. Experiments BarMar1-5 were used to calibrate and optimize
445 geometrical outline, deformation rate, and angles of relative plate movements
446 and are not shown here. The optimised geometries and experimental conditions
447 were utilised for experiments BarMar6-9, of which BarMar6 and 8 (and some
448 examples from BarMar9) are illustrated here. They yielded similar results in that
449 all crucial structural elements (faults and folds) were reproduced in all
450 experiments as described in the text (**Figure 4**). It is emphasized that the
451 extensional basins affiliated with the extension phase (phase 2) were wider for
452 the orthogonal (BarMar6) as compared to the oblique extension experiments
453 (BarMar 8) (**Figures 5 and 6**). Furthermore, the fold systems generated in the
454 experiments that utilised oblique contraction of $315/135^0$ (BarMar8-9)
455 produced more extensive systems of non-cylindrical folds. These folds also had
456 continuous, but more curved fold traces as compared to the experiments with
457 orthogonal extension/contraction (BarMar6). The fold axes generally rotated to
458 become parallel to the (extensional) master faults delineating the pull-apart
459 basins generated in deformation stage 1 in experiments with an oblique
460 opening/closing angle.

461 Examples of the sequential development are displayed in **Figures 5 and**
462 **6**, and summarised in **Figure 7**. Elongated positive structural elements with fold-
463 like morphology as seen on the surface were detected during the various stages
464 of the present experiments. The true nature of those were not easily determined
465 until the experiments were terminated and transects could be examined. Such
466 structures included buried push-ups (*sensu* Dooley & Schreurs, 2012), antiformal

467 **Table 1**
 468 Characteristics of Positive Structural Element (PSE 1-6) as described in the text and shown in figures. Note that the PSE-1-structures
 469 that were developed in the earliest stages of the experiments became cannibalised during the continued deformation. No candidates of
 470 these structures were identified in the reflection seismic sections.
 471

Struct. type	Structural configuration	Orientation	Expr. stage	Segment	Recognised in seismic	Figure Expr	Figure Seism
PSE-1	Open syn-anticline system	135 deg	Stage 1	1,3	?	5,6	1A?
PSE-2	Incipient flower or half-flower	Parallel master fault	Stage 1	1,2,3	Yes	5,6,8	1B
PSE-3	Forced folds above rotated fault blocks	Parallel master fault in releasing bend	Stage 2	1,2	Yes	9B	
PSE-4	Push-up	Parallel master fault in restraining bend	Stage 1	2	Yes	9D	1C
PSE-5	Anticlines/snake-heads in hanging walls	Parallel master faults	Stage 3	1,2,3	Yes	9C,D	1D,E
PSE-6	Anticline-syncline trains	Parallel master faults	Stage 3	1,2,3	Yes	12	1F

472



473

474 **Figure 5:** Sequential development of experiment BarMar6 by 0.5, 2.4, 3.5, 4.0 and 5.0 cm of dextral shear (Steps A-E), orthogonal
 475 extension (steps F-H) and oblique contraction (steps I-J). The master fault strands are numbered in **Figure 4**, and the sequential
 476 development for each structural family is shown in **Figure 7**. The reference panel to the upper left shows the positions of the segments.

477 stacks, back-thrusts, positive flower structures, fold trains, and simple anticlines.
478 For convenience, we use the non-genetic term “positive structural elements”
479 termed *PSEm-n* for such structure types as seen in the experiments in the
480 following description. In the following the deformation in each segment is
481 characterised for the three deformation phases (**Table 1**).

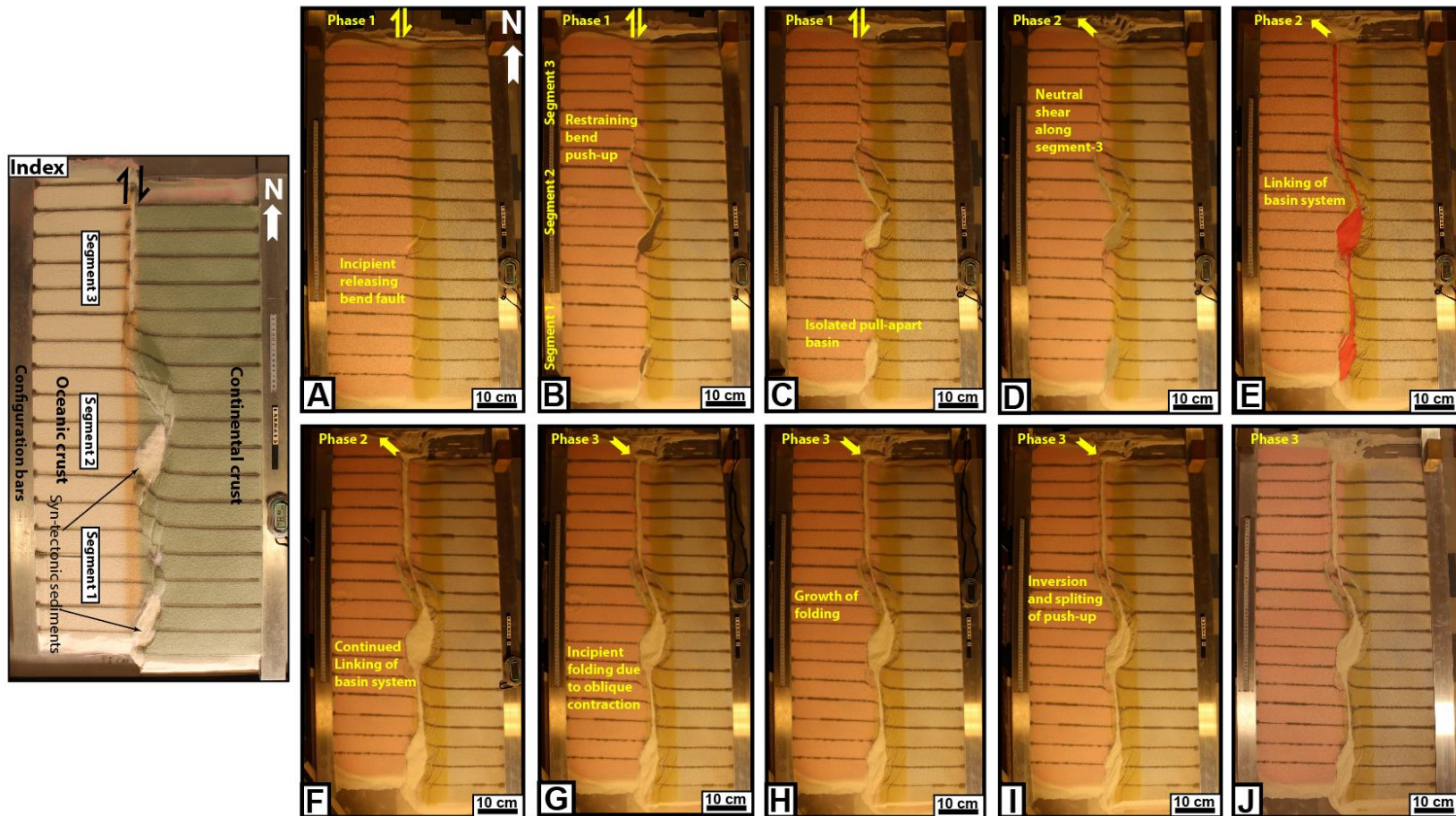
482

483 **Deformation phase 1: Dextral shear stage**

484 *Segment 1:* Differences in the geometry of the pre-cut fault trace between
485 segments 1, 2 and 3 became visible after the first deformation stage. In segments
486 1 and 3 in particular, an array of oblique *en échelon* folds between Riedel shear
487 structures (*PSE-1-structures*) oriented c. 135°(NW-SE) to the regional VD be
488 came visible before rotating towards NNW-SSE by continued shear (**Figure 8**;
489 see also Wilcox et al., 1973; Ordonne & Vialon, 1983; Richard et al., 1991; Dooley
490 & Schreurs, 2012). These were simple, harmonic folds with upright axial planes
491 and fold axial traces extending a few cm beyond the surface shear-zone
492 described above. They had amplitudes on the scale of a few millimeters and
493 wavelengths on scale of 5 cm. The *PSE-1-structures* interfered with or were
494 dismembered by younger structures (Y-shears and *PSE-2-structures*; see below)
495 causing northerly rotation of individual intra-fault zone lamellae (remnant *PSE-*
496 *1-structures*; **Figure 8**). Structures similar to *PSE-1-fold* arrays are known from
497 almost all strike-slip experiments reported and described in the literature (e.g.
498 Cloos, 1928; Riedel, 1929; See Dooley & Schreurs, 2012 for summary) and are
499 therefore not given further attention here.

500 By 0.25 cm of horizontal displacement in segment 1, which included releasing
501 and restraining bends separated by a central strand of neutral shear, a slightly
502 curvilinear surface trace of a NE-SW-striking, top-NW normal fault in the
503 southernmost part of segment 1 developed. This co-existed with the *PSE-1-*
504 *structures* and became paralleled by a normal fault with opposite dip (fault 2,
505 **Figure 4**) so that the two faults constrained a crescent- or spindle-shaped
506 incipient extensional shear duplex (**Figures 5B and 6B**; see also Mann et al.,
507 1983).

508 A system of separate *en échelon* N-S to NNE-SSE-striking normal and
509 shear fault segments became visible in segment 1 after ca. 1 cm of shear (**Figure**



510

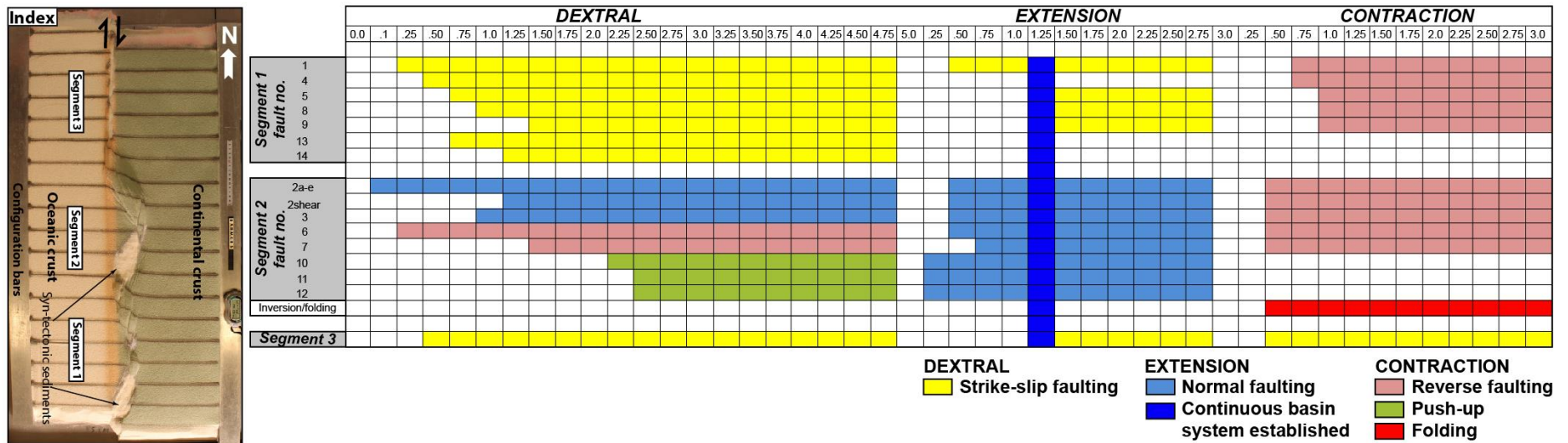
511 **Figure 6:** Sequential development of experiment BarMar8 by 0.5, 2.4, 3.5, 4.0 and 5.0 cm of dextral shear (Steps A-E), oblique extension
 512 (steps F-H) and oblique contraction (steps I-J). The master fault strands are numbered in **Figure 3**, and the sequential development for
 513 each structural family is shown in **Figure 7**. Phases 2 and 3 involved oblique (315°) extension and contraction in this experiment. The
 514 reference panel to the upper left shows the positions of the segments.

515 **5C,D**). These faults did not have the orientations as expected for R (Riedel) - and
516 R' (anti-Riedel)- shears (that would be oriented with angles of approximately 15
517 and 75° from the master fault trace) but became progressively linked with along
518 strike growth and the development of new faults and fault segments. They
519 thereby acquired the characteristics of Y-shears (oriented sub-parallel to the
520 master fault trace), dissecting the PSE-1-structures. By 2.4 cm of shear, segment
521 1 had become one unified fault array (**Figures 5D and 6D**), delineating a system
522 of incipient
523 push-ups or positive flower structures (*PSE-2-structures*; **Figures 8 and 10,**
524 **sections B1 and B3**).

525 The PSE-2-structures had amplitudes of 1 - 2 cm and wavelengths of 3 - 5
526 cm as measured on the surface with fault surfaces that steepened downward,
527 with the deepest parts of the structures having cores of sand-layers deformed by
528 open to tight folds. The folds had upright or slightly inclined axial planes, dipping
529 up to 55°, mainly to the east. The structures also affected the shallowest layers
530 down to 1-2 cm in the sequence, but the shallowest sequences developed at a
531 later stage of deformation and were characterised by simple gentle to open
532 anticlines. These structures were constrained to a deformation zone directly
533 above the trace of the basement fault, similar to that commonly seen along shear
534 zones (e.g. Tchalenko, 1971; Crowell, 1974 a,b; Dooley & Schreurs, 2012). This
535 zone was 3-4 cm wide and remained stable throughout deformation stage 1 and
536 was restricted to the close vicinity of the basement shear fault itself. A horse tail
537 like fault array developed by ca. 3 cm of shear at the transitions between
538 segments 1 and 2 (**Figures 5B-D and 6B-D**).

539 The structuring in *Segment 2* was determined by the pre-cut crescent-
540 shaped basement fault (velocity discontinuity) which caused the development of
541 a releasing bend along its southern, and a restraining bend along its northern
542 border (**Figure 11**). The first fault of fault array 3a-e in the southern part of
543 Segment 2 (**Figure 4**) was activated after c. 0.15 cm of bulk horizontal
544 displacement (**Figure 7**). It was situated directly above the southernmost pre-cut
545 releasing bend, defining the margin of crescent-shaped incipient extensional
546 strike-slip duplexes (in the context of Woodcock & Fischer, 1986, Woodcock &
547 Schubert, 1994 and Twiss & Moores, 2007, p. 140-141). The developing basin got

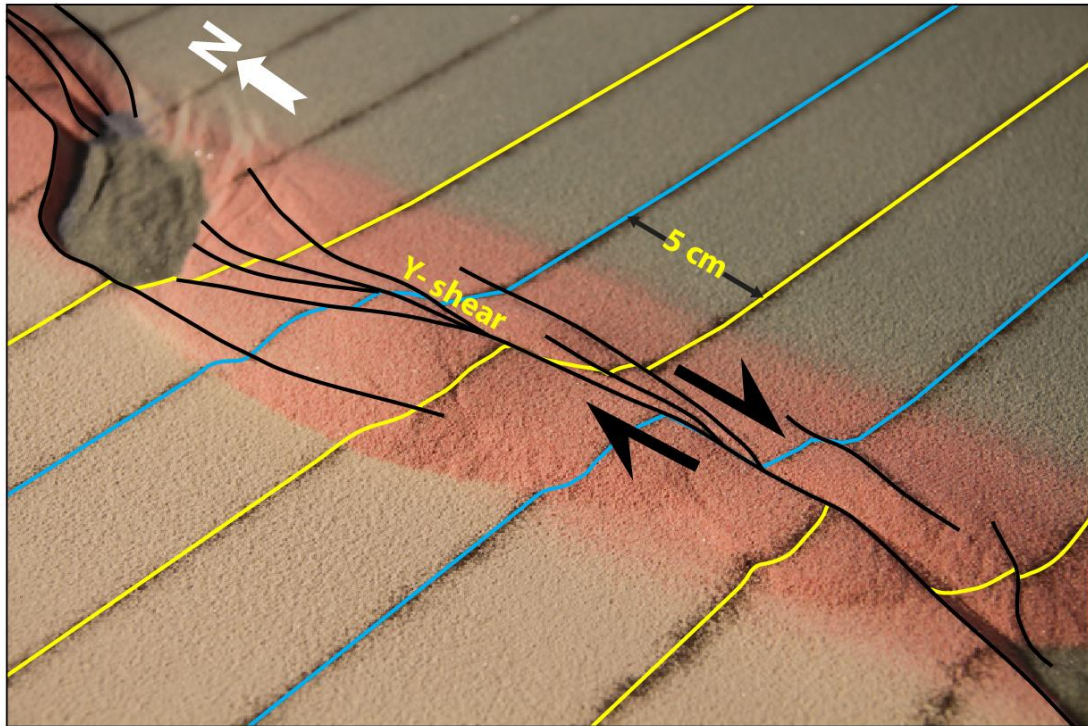
548



549 **Figure 7:** Summary of sequential activity in each master fault in Experiment BarMar6 (Figure 5) (for position of each fault, see Figure
550 4). Type and amount of displacement is shown in two upper horizontal rows. The vertical blue bar indicates the stage at which full
551 along-strike communication became established between marginal basins. Color code (see in-set) indicates type of displacement at any
552 stage. The reference panel to the left shows the positions of the segments.

553 a spindle-shaped structure and developed into a basin with a lazy-S-shape
554 (Cunningham & Mann, 2007; Mann, 2007). The basin widened towards the east
555 by stepwise footwall collapse, generating sequentially rotating crescent-shaped
556 extensional fault blocks that became trapped as extensional horses in the
557 footwall of the releasing bend (**Figure 11**). In the areas of the most pronounced
558 extension the crestal part of the rotational fault blocks became elevated above
559 the basin floor, generating ridges that influenced the basin floor topography and
560 hence, the sedimentation. By continued rotation of the fault blocks and
561 simultaneous sieving of sand the crests of the blocks became sequentially
562 uplifted, generating forced folds (Hamblin, 1965; Stearns, 1978; Groshong, 1989;
563 Khalil & McClay, 2016) (**Figure 10A**). In the analysis we used the term *PSE-3-*
564 *structures* for these features. Simultaneously, an expanding sand-sequence
565 became trapped in the footwalls of the master faults, defining typical growth-
566 fault geometries.

567 By a shear displacement of 0.55 cm additional curved splay faults were initiated
568 from the northern tip of the master fault of fault 3f; **Figure 7**), delineating the
569 northern margin of a rhombohedral pull-apart-basin (Mann et al., 1983; Mann,
570 2007; Christie-Blick & Biddle, 1985) and with a geometry that was
571 indistinguishable from pull-apart basins or rhomb grabens affiliated with
572 unbridged *en échelon* fault arrays (Crowell, 1974 a,b; Aydin & Nur, 1993).
573 Although sand was filled into the subsiding basins to minimize the graben relief
574 and to prevent gravitational collapse, the sub-basins that were initiated in the
575 shear-stage were affected by internal cross-faults, and the initial basin units
576 remained the deepest so that the buried internal basin topography maintained a
577 high relief with several apparent depo-centers separated by intra-basinal
578 platforms. Systems of linked shear faults and PSE-structures became established
579 in the central part with neutral shear that separate the releasing and restraining
580 bends and development similarly to that seen for segment 3 (see below). These
581 structures were, however, soon destroyed by the interaction between the
582 northern and southern tips of the extensional and contractional shear duplexes
583 (**Figure 10**).



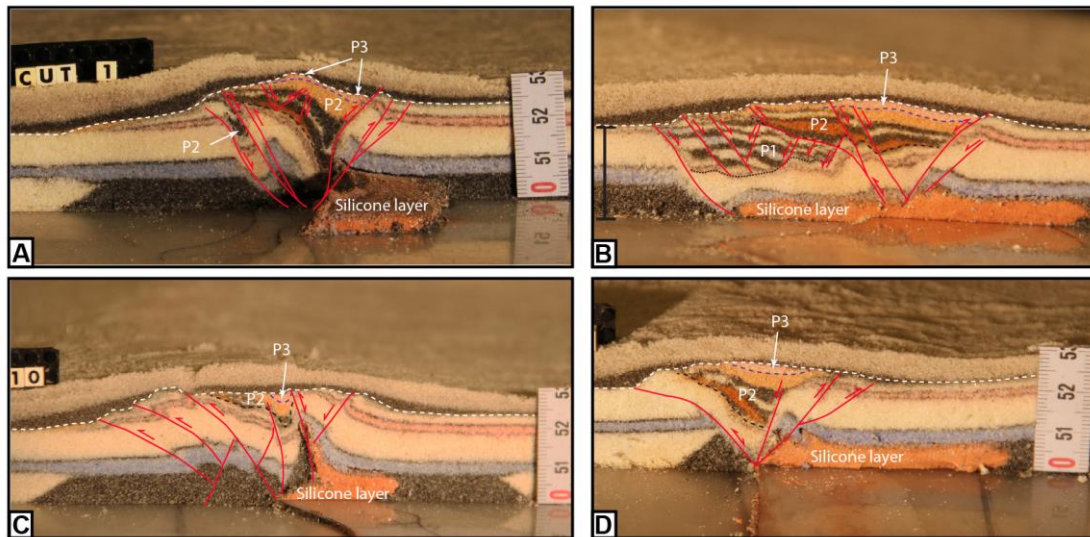
584

585 **Figure 8:** PSE-1 anticline-syncline pairs in segment 1 of experiment BarMar6
 586 in an oblique view (see **Figure 4** for position of Segment 1). PSE-1 folds (indicated
 587 by relief defined by blue and yellow markers) were constrained to the central
 588 fault zone (defined by Y-shear and its splay faults) and extended only 3-4 cm
 589 beyond it. PSE-2 structures (incipient push-ups and positive flower structures)
 590 were delineated by shear faults (black lines) and completely cannibalised PSE-1
 591 structures by continued shear. Yellow and blue reference lines illustrate the
 592 rotation of the fold axial trace caused by dextral shear. Already pre-shear
 593 distance between the markers (blue and yellow lines) was 5cm. Black arrow
 594 indicates shear direction.

595

596 The first structure to develop in the regime of the restraining bend (segment 2;
 597 was a top-to-the-southwest (antithetic) thrust fault at an angle of 145° with the
 598 regional trend of the basement border as defined by segments 1 and 3 (Fault 6).
 599 It became visible by 0.5 cm of displacement. However, the northern part of
 600 segment 2 became dominated by a synthetic contractional top-to-the-northeast
 601 fault that was initiated by 0.85 cm of shear (Fault 7; **Figures 5 and 6**). Thus,
 602 faults 6 and 7 delineated a growing half-crescent-shaped 5-7 cm wide push-up
 603 structure (Aydin & Nur, 1982; Mann et al., 1983) south of the restraining bend
 604 (**Figure 9**; PSE-4-structures). Continued shearing gave these structures the
 605 character of an antiformal stack.

606 *Segment 3* defined a straight strand of neutral shear. Its development in
 607 the BarMar-experiments followed strictly that known from numerous published

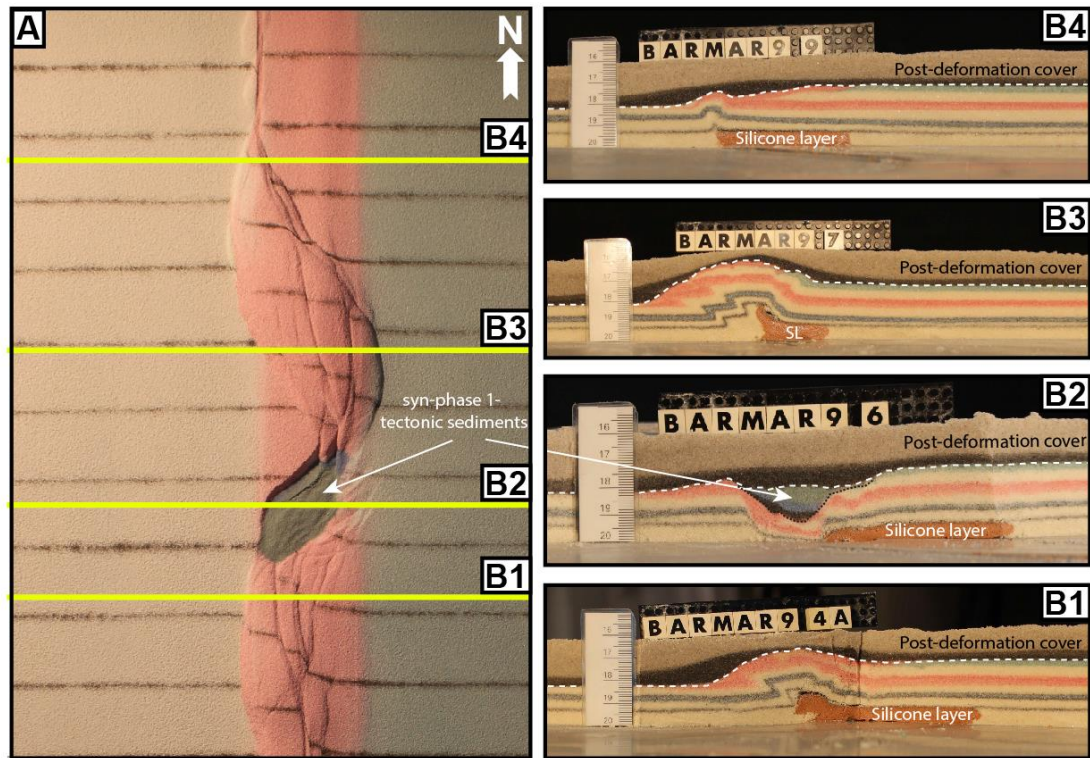


608

609 **Figure 9:** Cross-sections through PSE-2-related structures. PSE-structures are
 610 marked with P and PSE-number as described in text (see also Table 1). **A)**
 611 Folded core of incipient push-up/positive flower structure in segment 1,
 612 experiment BarMar6. The fold structure is completely enveloped of shear faults
 613 that have a twisted along-strike geometry. Note that the eastern margin of the
 614 structure developed into a negative structure at a late stage in the development
 615 (filled by black-pink sand sequence) and that the silicone putty sequence (basal
 616 pink sequence) was entirely isolated in the footwall. **B)** Similar structure type in
 617 experiment BarMar8. However, the basal silicone putty layer here bridged the
 618 basal high-strain zone so that folding occurred in the footwall as well as in the
 619 hanging. Folds propagated up-section into the sand layers (blue). The folds in
 620 upper (pink) layers are younger and were associated with the contractional
 621 stage (PSE-6-structures). **C)** Contraction associated with “crocodile structure” in
 622 the footwall of the main fault in segment 1, experiment BarMar8. Note
 623 disharmonic folding with contrasting fold geometries in hanging wall and
 624 footwall and at different stratigraphic levels in the footwall, indicating that
 625 shifting stress situation in time and space occurred in the experiment. **D)**
 626 Transitional fault strand between to more strongly sheared fault segments
 627 (experiment BarMar9).

628

629 experiments (e.g. Tchalenko, 1970; Wilcox et al., 1973; Harding, 1974; Harding &
 630 Lowell, 1979; Naylor et al., 1986; Sylvester, 1988; Richard et al., 1991; Woodcock
 631 & Schubert, 1994; Dauteuil & Mart, 1998; Mann, 2007; Casas et al., 2001; Dooley
 632 & Schreurs, 2012). A train of Riedel-shears, occupying the full length of the
 633 segment, appeared simultaneously on the surface after a shear displacement of
 634 0.5 cm, occupying a restricted zone with a width of 2-3 cm. The Riedel-shears
 635 dominated the continued structural development of Segment 3. Riedel'-shears
 636 were absent throughout the experiments, as should be expected for a sand-
 637 dominated sequence (Dooley & Schreurs, 2012). P-shears developed by



638

639 **Figure 10: A)** Contrasting structural styles along the master fault system in
 640 segment 2 in map view and **(B)** cross sections of experiment BarMar9. SL
 641 denotes silicone layer, the stippled line the boundary between pre- and syn-
 642 deformation layers and the white dashed line the boundary with the post-
 643 deformation layers.
 644

645 continued shear, creating linked rhombic structures delineated by the Riedel-
 646 and P-shears generating positive structural elements with NW-SE- and NNE-SSE-
 647 striking axes (see also Morgenstern & Tchalenko, 1967), soon coalescing to form
 648 Y-shears. Transverse sections document that these structures were cored by
 649 push-up anticlines, positive half-flower structures and full-fledged positive
 650 flower structures in the advanced stages of shear (*PSE-4-structures*) (**Figures 5**
 651 **and 6; See also Figure 10**). These were accompanied by the development of *en*
 652 *échelon* folds and flower structures as commonly reported from strike-slip faults
 653 in nature and in experiments. The width of the zone above the basal fault
 654 remained almost constant throughout the experiments, but was somewhat wider
 655 in experiments with thicker basal silicone polymer layers, similar to that
 656 commonly described from comparable experiments (e.g. Richard et al., 1991).

657

658

659 **Deformation Phase 2: Extension**

660 The late Cretaceous-Palaeocene dextral shear was followed by pure extension
661 that accompanied the opening along the Barents Shear Margin in the Oligocene.
662 Our experiments focused on the effects of oblique extension, acknowledging that
663 plate tectonic reconstructions of the North Atlantic suggest an extension angle of
664 315° (Gaina et al., 2009).

665 All strike-slip basins widened in the extensional stage and as one would
666 expect, the basins generated in orthogonal extension became wider than those
667 generated in oblique extension. In both cases, however, extension promoted
668 enhanced relief that had been generated in the shear-stage. In the earliest
669 extensional stage, the strike-slip basin in segment 2 dominated the basin
670 configuration. By continued extension the linear segments and the minor pull-
671 apart basins in segments 1 and 2 started to open and became interlinked,
672 subsequently generating a linked basin system that runs parallel to the entire
673 shear margin (**Figures 5F-G, 6F-G**). The basins had become completely
674 interlinked by an extension of 1.25 cm (marked by the vertical dark blue line in
675 **Figure 7**). The orthogonal extension-phase also reactivated and linked several
676 master faults that were established in deformation phase 1 (**Figures 5A and**
677 **6A**). This became evident by an extension of 0.25 – 0.50 cm and included the
678 southern fault margin, the push-up and the splay faults defining the crestal
679 collapse graben (Faults 6, 11 and 12; **Figure 4**). Among the faults that remained
680 inactive throughout the extension phase were the antithetic contractional fault
681 delineating the push-ups in segment 2 (Fault 6; **Figure 4**). The Y-shear in
682 Segment 3 was reactivated as a straight, continuous extensional fault in phase 2.
683 Total extension in stage 2 was 5 cm.

684

685 **Deformation Phase 3: contraction**

686 In our experiments the extension stage was followed by oblique contraction (
687 parallel to the direction of extension as applied for each experiment). A part of
688 the early-stage contraction was accommodated along new faults. More
689 commonly, however, faults that had been generated in the strike-slip and
690 extensional stages became reactivated and rotated. So was the development of
691 isolated folds, which were commonly associated with inverted fault traces,

692 generating snake-head or harpoon-structures structures (Cooper et al., 1989;
693 Coward, 1994; Allmendinger, 1998; Yameda & McClay, 2004; Pace & Calamitra,
694 2014; *PSE-5-structures*). The predominant structures affiliated with the
695 contractional stage were still new folds with traces oriented orthogonal to the
696 shortening direction and subparallel to the preexisting master fault systems that
697 defined the margin and basin margins (**Figure 12**). Also, some deep fold sets that
698 had been generated during the strike-slip phase and seen as domal surface
699 features became reactivated, causing renewed growth of surface structures (see
700 **Figure 10** and explanation in figure caption). These folds were generally up-
701 right cylindrical buckle folds in the initial contractional and with very large trace
702 to amplitude-ratio (*SPE-6-structures*). Some intra-basin folds, however, defined
703 fold arrays that crossed the basins in a diagonal fashion. Particularly the folds
704 situated along the basin margins developed into fault propagation-folds above
705 low-angle thrust planes. Such faults aligning the western basin margins could
706 have an antithetic attitude relative to the direction of contraction.

707 During the contractional phase the margin-parallel, linked basin system
708 started immediately to narrow and several fault strands became inverted. The
709 basin-closure was a continuous process until the end of the experiment by 3 cm
710 of contraction. The contraction was initiated as a proxy for an ESE-directed
711 ridge-push stage. The first effect of this deformation stage was heralded by uplift
712 of the margin of the established shear zone that had developed into a rift during
713 deformation stage 2. This was followed by the reactivation and inversion of
714 some master faults (e.g. fault a2; **Figure 4**) and thereafter by the development of
715 a new set of low-angle top-to-the-ESE contractional faults. These faults displayed
716 a sequential development (fault family 1; **Figure 7**) and were associated with
717 folding of the strata in the rift structure, probably reflecting foreland-directed in-
718 sequence thrusting (*SPE-5* and *PSE-6* fold populations).

719

720 **Discussion**

721 The break-up and subsequent opening of the Norwegian-Greenland Sea was a
722 multi-stage event (**Figure 13**) that imposed shifting stress configurations
723 overprinting the already geometrically complex Barents Shear Margin.
724 Therefore, scaled experiments were designed to illuminate its structural

725 development. The experiments utilised three main segments that correspond to
726 the Senja Fracture Zone (segment 1), the Vestbakken Volcanic Province (segment
727 2) and the Hornsund Fault Zone (segment 3) respectively and three deformation
728 phases (dextral shear, oblique extension and contraction). Several structural
729 families (PSE 1-6) generated in the experiments correspond to structural
730 features observed in reflection seismic sections. In the following discussion we
731 utilize these two data sets in explaining the sequential development of each
732 segment of the shear margin.

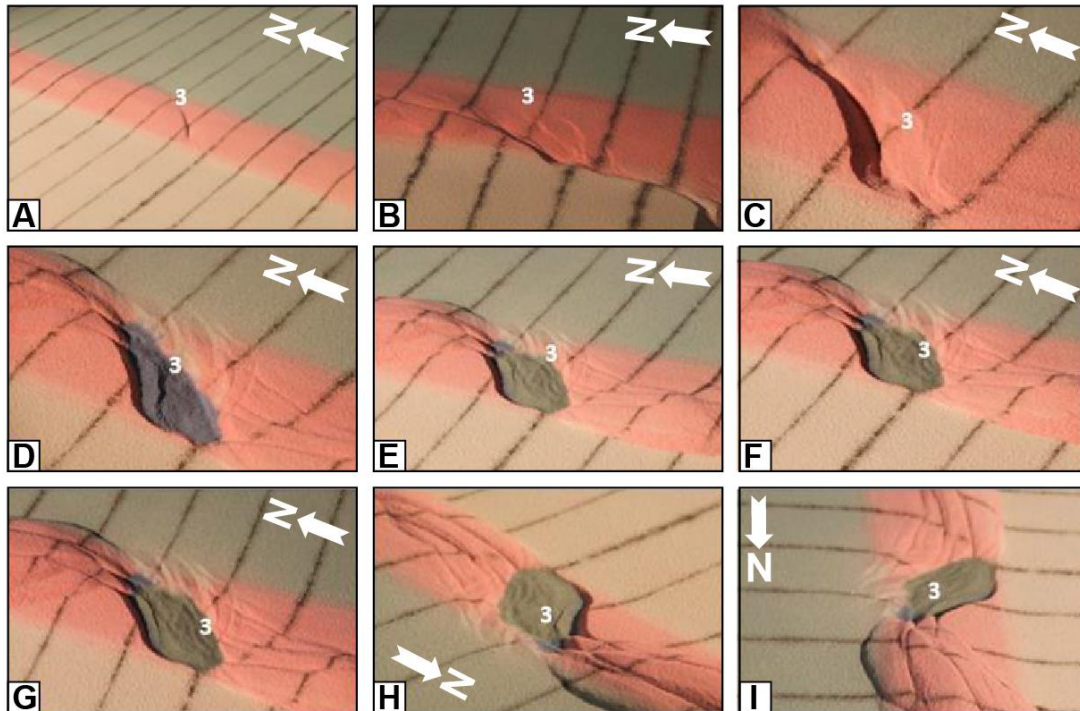
733

734 **Structures of phase 1 (dextral shear)**

735 *Segment 1* (corresponding to the Senja Fracture Zone) was dominated by neutral
736 dextral shear, although jogs in the (pre-cut) fault provided minor sub-segments
737 with subordinate releasing and restraining bends.

738 PSE-1-folds seen in the incipient shear phase were confined to the area just
739 above the basal master fault (VD) and its immediate vicinity (see also
740 experiments in series “e” and “f” of Mitra & Paul, 2011). Counterparts to PSE-1
741 structural population were not identified in the seismic data, although some
742 isolated, local anticlinal features could be dismembered remnants of such.
743 Because of their constriction to the near vicinity of the master fault it is
744 reasonable that structures generated at an early stage of shear are vulnerable to
745 cannibalization by younger structures with axes striking parallel to the main
746 shear fault (Y-shears; SPE-2-structures). We therefore conclude that this
747 structure population was destroyed during the later stages of shear and during
748 the subsequent stages of extension and contraction. PSE-1-folds that developed
749 at an incipient stage were immediately pursued by the development of two sets
750 of NNE-SSW-striking normal faults with opposite throws in the releasing bend
751 areas (e.g. fault 2 **Figure 4**). The two faults defined crescent- or spindle-shaped
752 incipient extensional shear duplexes. These structures were stable during the
753 remainder of the experiments and their master faults became reactivated during
754 the extensional and contractional phases (see below). The most prominent of
755 these structures corresponds to the position of the Sørvestsnaget Basin (**Figure**
756 **1B**).

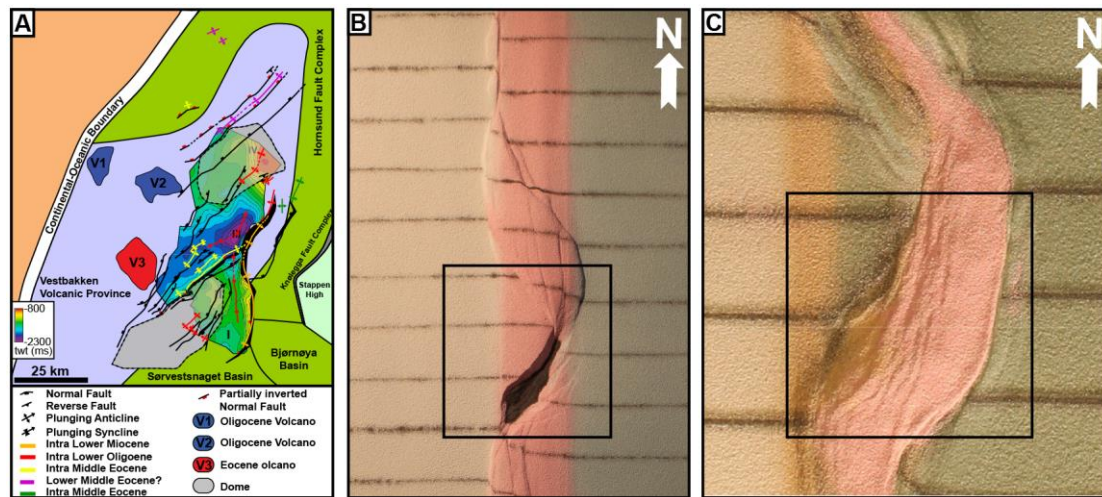
757



758

759 **Figure 11:** Nine stages in the development of the extensional shear duplex
 760 system above the releasing bend in experiment BarMar9. The master faults that
 761 developed at an incipient stage (e.g. Fault 3 that constrained the eastern margin
 762 of the extensional shear duplex, marked with "3" in the figure; see also **Figure 7**)
 763 remained stable and continued to be active throughout the experiment, but
 764 became overstepped by new faults in its footwall. These were reactivated as
 765 contraction faults at the later stages (stages H and I in this figure). The
 766 developing basement was stabilised by infilling of gray sand during this part of
 767 the experiment. Fault 3 continued to breach the basin infill also after the basin
 768 infill overstepped the original basin margin. The distance between the markers
 769 (dark lines) is 5cm. White arrow marks north-direction. Note that figures "H"
 770 and "I" (bottom right) is viewed from directions than the other figures.
 771

772 *Segment 2*, which was controlled by a pre-cut crescent-shaped discontinuity in
 773 the experiments corresponds to the Vestbakken Volcanic Province and the
 774 southern extension of the Knølegga Fault Complex of the Barents Shear Margin
 775 (**Figures 1B and 4**). The Vestbakken Volcanic Province is dominated by
 776 interfering NNW-SSE- and NE-SW striking fold- and fault systems in its central
 777 part, whereas N-S-structures are more common along its eastern margin (**Figure**
 778 **12A**) (Jebsen & Faleide, 1998; Giannenas, 2018). Intra-basinal highs and other
 779 internal configurations seen in the BarMar-experiments mainly reflect step-wise
 780 collapse of the intrinsic basin that generated rotational fault blocks, the crests of
 781 which separated local sediment accumulations.



782

783 **Figure 12:** PSE-5-folds generated during phase 3-inversion, experiment
 784 BarMar8. Note that fold axes are mainly parallel the basin rims, but that they
 785 deviate in some cases in the central parts of the basins.. The folds are best
 786 developed in segment 2, which accumulated extension in the combined shear
 787 and extension stages.

788

789 Such structures are common in strike-slip basins (e.g. Dooley & McClay, 1997;
 790 Dooley & Schreurs, 2012) and are consistent with the intra-basin depo-centers
 791 seen within the Vestbakken Volcanic province and in the Sørvestsnaget Basin as
 792 well (Knutsen & Larsen, 1997; Jebesen & Faleide, 1998; **Figure 13**). The crests of
 793 the rotating fault blocks are termed PSE-3-structures above, and such eroded
 794 fault block crests are defining the footwalls of major faults in the Vestbakken
 795 Volcanic Province, providing space for sediment accumulation in the footwalls.
 796 The area that was affected by the basin formation in the extensional shear
 797 duplex stage seems to have remained the deepest part of the Vestbakken
 798 Volcanic Province. The part formed by basin widening through sequential
 799 footwall collapse formed a shallower subplatform (*sensu* Gabrielsen, 1986)
 800 (**Figure 11**).

801

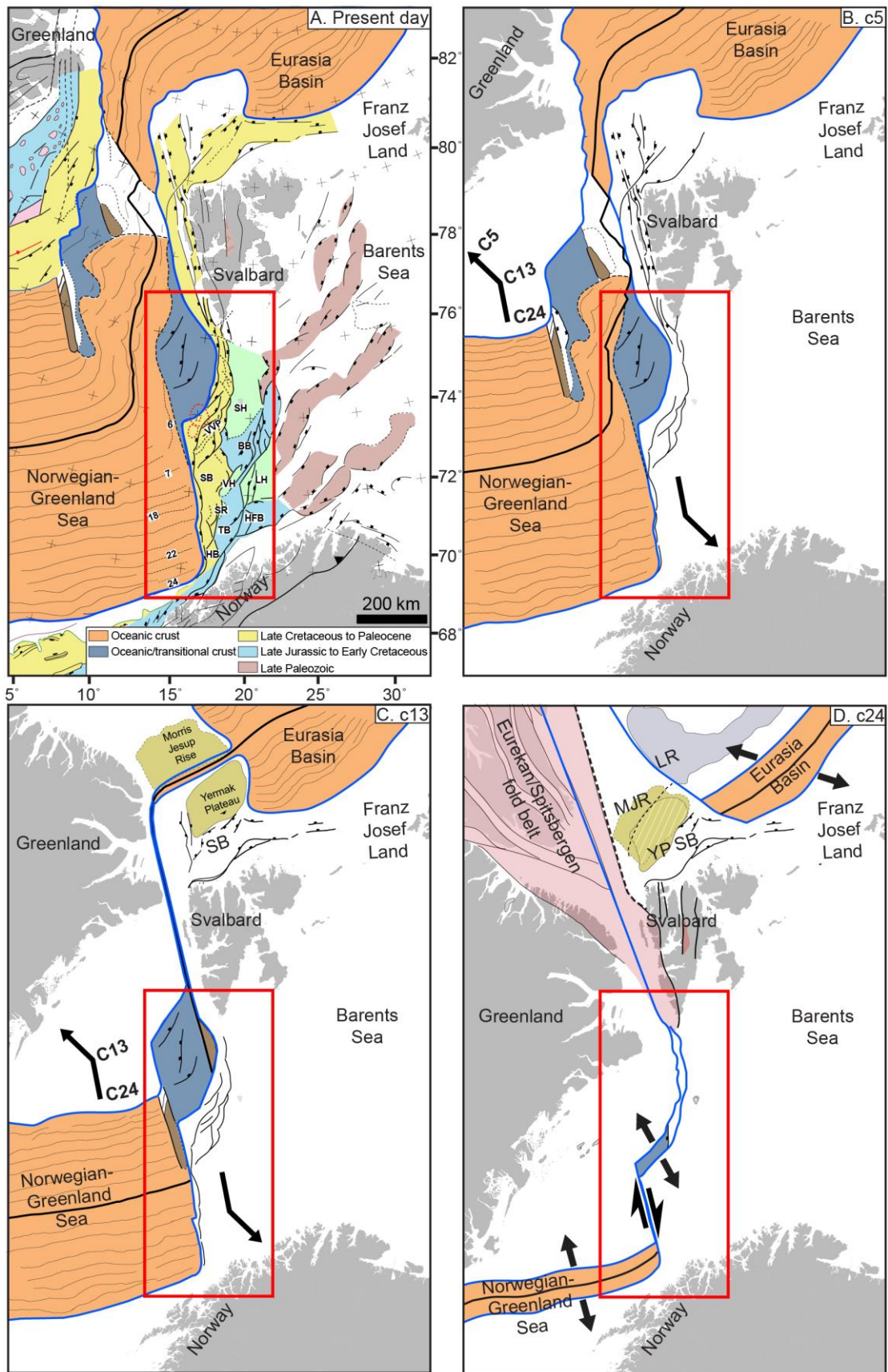
802 The Knølegga Fault Complex occupies a km-wide zone in segment 2. The
 803 master fault strand is paralleled by faults with significant normal throws in its
 804 hanging wall side and is a part of the larger Knølegga Fault Complex (EBF;
 805 Eastern Boundary Fault; Giannenas, 2018; **Figure 12A**). The EBF zone is a top-
 806 west normal fault with maximum throw of nearly 3000 meters. It can be
 807 followed along its strike for more than 60 km and seems to die out by horse-
 808 tailing at its tip-points. The vicinity of the master faults of the Knølegga Fault
 Complex locally display isolated elongate positive structures constrained by

809 steeply dipping faults. These structures sometimes display internal reflection
810 patterns that seem exotic in comparison to the surrounding sequences. Some of
811 these structures resemble positive flower structures or push-ups or define
812 narrow anticlines. They are located in both the footwall and hanging wall of the
813 boundary faults and strike parallel to them and the axes of these structures are
814 parallel the master faults. The traces of such structures can be followed over
815 shorter distances than the master faults, and do not occur in the central parts of
816 the Vestbakken Volcanic Province. We suggest that the composite geometry of
817 the Knølegga Fault Complex is due to the development of PSE-2-structures
818 within the realm of a pre-existing normal fault zone.

819 Due to the right-stepping geometry during dextral shear in segment 2, the
820 southern and northern parts were in the releasing and restraining bend
821 positions, respectively (e.g. Christie-Blick & Biddle, 1985). Hence, the southern
822 part of segment 2 was subject to oblique extension, subsidence and basin
823 formation while the northern part was subject to oblique contraction, shortening
824 and uplift. The southern segment expanded to the east and northeast by footwall
825 collapse and activation of rotating fault blocks that contributed to a basin floor
826 topography that affected the pattern of sediment accumulation (**Figure 9A,B**).

827 The positive structural elements that prevail in *segment 3* belong to the
828 PSE-2-structure population. The structures affiliated with segment 3 in the
829 BarMar-experiments are similar to those seen in the reflection seismic sections
830 along parts of the Spitsbergen and the Senja shear margins (Myhre, et al. 1982)
831 and elsewhere (Cloos, 1928; Riedel, 1929; Tchalenko, 1970; Wilcox et al., 1973).
832 In the experiments *en echelon* folds (corresponding to PSE-1-structures) first
833 became visible, to be succeeded by the development of Riedel- and P-shears (R'-
834 shears were subdued as expected for sand-dominated sequences (Dooley &
835 Schreurs, 2012). Continued shear followed by collapse and interaction between
836 Riedel and P-shears and the subsequent development of Y-shears initiated push-
837 up- and flower-structure with N-S-axes (PSE-2) structures that were expressed
838 as non-cylindrical (double-plunging) anticlines on the surface (e.g. Tchalenko,
839 1970; Naylor et al., 1986). Structures similar to the PSE-2-structures that were
840 initiated in the present experiments are common in scaled experiments with

841



842

843 **Figure 13;** Main stages in opening of the North Atlantic. The figure builds on
 844 figure 5 in Faleide et al. (2008) and has been updated and redrawn.

845

846 mechanically stratified sequences where viscous basal strata are covered by
847 sand (e.g. Richard et al., 1991; Dauteuil & Mart, 1998).

848

849 **Structures of phase 2 (extension)**

850 It is expected that (regional) basin and (local) fault block subsidence became
851 accelerated during phase 2 (extension), and more so in the orthogonal extension
852 experiments (BarMar 6) than in the experiments with oblique extension (BarMar
853 8). However, due to stabilization of basins by infilling of sand, this was not
854 documented in the final photographs. The widening occurred mainly by fault-
855 controlled collapse of the footwalls, and dominantly along the master faults that
856 correspond to the Knølegga Fault Complex. However, new transverse fault
857 within the basin that had developed during the shear stage (see above) were also
858 reactivated and contributed to the complexity of the basin topography. It is
859 unlikely that a stage was reached where all (pull-apart) basin units along the
860 margin became fully linked, although sedimentary communication along the
861 margin may have occurred.

862 During the oblique extension stage segment 1 of experiments BarMar7-9
863 the basin subsidence was focused in the minor pull-apart basins, which soon
864 became linked along the regional N-S-striking basin axis. Remains of several such
865 basin centers, of which the Sørvestsnaget Basin (Knutsen & Larsen, 1997;
866 Kristiansen et al., 2017) is the largest, are preserved and found in seismic data
867 (**Figure 1B**). During the experiments a continuous basin system was developed
868 in the hanging wall side of the master fault. It is, however, not likely that linking
869 of shear basins occurred prior to the opening stage along the Barents Shear
870 Margin.

871

872 **Structures of phase 3 (contraction)**

873 The contraction phase (phase 3) reactivated both normal and shear faults in the
874 master fault zone also causing folding in the hanging wall. Simultaneously
875 rotation of (intra-basinal) fault blocks and steepening of pre-existing faults
876 occurred. New fold populations (PSE-5-folds) with axial traces parallel to the
877 basin axis and the master faults characterised the inversion stage. Remnants of

878 such folds are locally preserved in the thickest sedimentary sequences affiliated
879 with the Senja Shear Margin.

880 Fold systems with fold axes paralleling the basin margins as seen in the
881 experiments are also common in the Vestbakken Volcanic Province. Although
882 shortening occurred inside individual reactivated fault blocks by large
883 wavelength bulging of the entire sedimentary sequence also trains of folds with
884 larger amplitude and shorter wavelength were developed at this stage (**Figure**
885 **12B,C**). Thus, the tectonic inversion was focused along the N-S-striking basin
886 margins but also occurred along some pre-existing NE-SW-striking faults and in
887 the central parts of the basin.

888 During phase 3 the restraining bend configuration in the northern part of
889 segment 2 was characterised by increasing contraction across strike-slip fault
890 strands that splayed out to the northwest from the central part of segment 2 in
891 an early stage of dextral shear. This deformation was terminated by the end of
892 phase 1 by stacking of oblique contraction faults (PSE-5 and PSE-6-structures),
893 defining an antiformal stack-like structure. This type of deformation falls outside
894 the mapped area, but to the north this type of oblique shortening during the
895 Eocene (phase 1) was accommodated by regional-scale strain partitioning
896 (Leever et al., 2011a,b).

897 Also, the Vestbakken Volcanic Province is characterised by extensive
898 regional shortening. Onset of this event of inversion/contraction is dated to early
899 Miocene (Jebsen & Faleide, 1998, Giannenas, 2018) and this deformation
900 included two main structural fold styles. The first includes upright to steeply inclined,
901 closed to open anticlines that are typically present in the hanging wall of master
902 faults. These folds typically have wavelengths in the order of 2.5 to 4.5 kilometers
903 and amplitudes of several hundred meters. Most commonly they appear with head-on
904 snakehead-structures and are interpreted as buckle folds, albeit a component of shear
905 may occur in the areas of the most intense deformation. The second style includes
906 gentle to open anticline-syncline pairs with upright or steep to inclined axial planes
907 with wavelengths on the order of 5 to 7 kilometers and amplitudes of several tens of
908 meters to several hundred meters. We associate those with the PSE-4-type structures
909 as defined in the BarMar-experiments. These folds are situated in positions where
910 sedimentary sequences have been pushed against buttresses provided by master faults

911 along the basin margins. The PSE-6 folds developed as fold trains in the interior
912 basins, where buttressing against larger fault walls was uncommon. Also, this pattern
913 fits well with the development and geometry seen in the BarMar-experiments, where
914 folding started in the central parts of the closing basins before folding of the marginal
915 parts of the basin. In the closing stage the folding and inversion of master faults
916 remained focused along the basin margins.

917 The experiments clearly demonstrated that contraction by buckle folding
918 was the main shortening mechanism of the margin-parallel basin system
919 generated in phase 2 (orthogonal or oblique extension) in all segments. In the
920 Vestbakken Volcanic Province segments of the Knølegga Fault Complex, the EBF
921 and the major intra-basinal faults contain clear evidence for tectonic inversion,
922 whereas this is less pronounced in others. The hanging wall of the EBF is partly
923 affected by fish-hook-type inversion anticlines (Ramsey & Huber, 1987; Griera et
924 al., 2018) (**Figure 2D,E**), or isolated hanging wall anticlines or pairs or trains of
925 synclines and anticlines (e.g.; Roberts, 1989; Coward et al., 1991; Cartwright,
926 1989; Mitra, 1993; Uliana et al., 1995; Beauchamp et al. 1996; Gabrielsen et al.
927 1997; Henk & Nemcok 2008), the fold style and associated faults probably being
928 influenced by the orientation and steepness of the pre-inversion fault (Williams
929 et al., 1989; Cooper et al., 1989; Cooper & Warren, 2010). Some structures of this
930 type can still be followed for many kilometers having consistent geometry and
931 attitude. These structures are not much modified by reactivation and are
932 invariably found in the proximal parts footwalls of master faults, suggesting that
933 these are inversion structures. They correlate to PSE-type 5-structures in the
934 experiments that developed in areas of focused contraction along pre-existing
935 fault scarps during Oligocene inversion.

936 Trains of folds with smaller amplitudes and higher frequency are
937 sometimes found in fault blocks in the central part of the Vestbakken Volcanic
938 Province (**Figure 12A**). Although these structures cannot be dated by seismic
939 stratigraphical methods (on-lap configurations etc.) we assume that these folds
940 can be correlated with the tight folds generated in the inversion stage in the
941 experiments (PSE-6-structures) and that they are contemporaneous with the
942 PSE-5-structures.

943 Segment 1 in the experiments, that corresponds to the Senja Shear
944 Margin, displays a structural pattern that is a hybrid between segments 1 and 2:
945 It contains incipient structural elements that were developed in full in segments
946 2 and 3, segment 2 being dominated by releasing and restraining bend
947 configurations and segment 3 dominated by neutral shear. Because of internal
948 configurations, the three segments were affected to secondary (oblique) opening
949 and contraction in various fashions. Understanding these differences was much
950 promoted by the comparison of seismic and model data.

951

952 **Some considerations about multiphase deformation in shear margins**

953 The Barents Shear Margin is a challenging target for structural analysis both
954 because it represents a geometrically complex structural system with a
955 multistage history, but also because high-quality (3D) reflection seismic data are
956 limited and many structures and sedimentary systems generated in the earlier
957 tectono-thermal stages have been overprinted and obliterated by younger
958 events. This makes analogue experiments very useful in the analysis, since they
959 offer a template for what kind of structural elements can be expected. By
960 constraining the experimental model according to the outline of the margin
961 geometry and introducing a dynamic stress model consistent with according to
962 the current understanding of the tectono-sedimentological evolution, we were
963 able to interpret the observations done from the reflection seismic data in a new
964 light.

965 Continental margins are commonly segmented containing primary or
966 secondary transform elements, and pure strike-slip transforms are relatively
967 rare (e.g. Nemcok et al. 2016). Such margins, however, invariably become
968 affected by extension following break-up and sometimes contraction due to
969 ridge-push or far-field stress perhaps related to plate reorganization. The
970 complexity of shear margins has ignited several conceptual discussions. One
971 such discussion concerns the presence of zones of weakness prior to break-up
972 (e.g. Sibuet & Mascle 1978; Taylor et al, 2009; Gibson et al. 2013; Basile 2015). In
973 the case of the Barents Shear Margin the de Geer zone provides such a pre-
974 existing zone of weakness, and this premise was acknowledged when the scaled
975 model was established. The relevance of our model is therefore constrained to

976 cases where a crustal-scale zone of weakness existed before break-up.
977 Furthermore, in cases with pre-existing zones of weakness, our model shows
978 that the initial architecture of the margin is indeed important indeed and the
979 detailed geometry and width of the pre-existing weak zone must be mapped and
980 included in the model.

981

982 **Summary and conclusions**

983 Our observations confirmed that the main segments of the Barents Shear Margin,
984 albeit undergoing the same regional stress regime, display contrasting structural
985 configurations. The deformation in segment 2 in the BarMar-experiments, was
986 determined by releasing and restraining bends in the southern and northern
987 parts, respectively. Thus, the southern part, corresponding to the Vestbakken
988 Volcanic Province, was dominated by the development of a regional-scale
989 extensional shear duplex as defined by Woodcock & Fischer (1983) and Twiss &
990 Moores (2007). By continued shear the basin developed into a full-fledged pull-
991 apart basin or rhomb graben (Crowell, 1974; Aydin & Nur, 1982) in which
992 rotating fault blocks were trapped. The pull-apart-basin became the nucleus for
993 greater basin systems to develop in the following phase of extension also
994 providing the space for folds to develop in the contractional phase.

995 We conclude that fault- and fold systems found in the realm of the
996 Vestbakken Volcanic Province are in accordance with a three-stage development
997 that includes dextral shear followed by oblique extension and contraction
998 ($315/135^{\circ}$) along a shear margin with composite geometry. Folds with NE-SW-
999 trending fold axes are dominant in wider area of the Vestbakken Volcanic
1000 Province and are dominated by folds in the hanging walls of (older) normal
1001 faults, sometimes characterised by narrow, snake-head- or harpoon-type
1002 structures that are typical for tectonic inversion (Cooper et al., 1989; Coward,
1003 1994; Allmendinger, 1998; Yameda & McClay, 2004; Pace & Calamitra, 2014).

1004 Comparison of seismic mapping and analogue experiments shows that
1005 one of the major challenges in analysing the structural pattern in shear margins
1006 of complex geometry and multiple reactivation is the low potential for
1007 preservation of structures formed in the earliest stages of development.

1008

1009 **Author contribution**

1010 R.H.Gabrielsen: Contributions to outline, design and performance of
1011 experiments. First writing and revisions of manuscript. First drafts of figures.

1012 P.A.Giannenas: Seismic interpretation in the Vestbakken Volcanic Province.
1013 Identification and description of fold families.

1014 Suggestion:

1015 D.Sokoutis: Main responsibility for set-up, performance and handling of
1016 experiments. Revisions of manuscript.

1017 E.Willigshofer: Performance and handling of experiments. Revisions of
1018 manuscript. Design and revisions of figure material.

1019 M. Hassaan: Background seismic interpretation. Discussions and revisions of
1020 manuscript. Design and revisions of figure material.

1021 J.I.Faleide: Regional interpretations and design of experiments. Participation in
1022 performance and interpretations of experiments. Revisions of manuscript,
1023 design and revisions of figure material.

1024

1025 **Acknowledgements**

1026 The work was supported by ARCEX (Research Centre for Arctic Petroleum
1027 Exploration), which was funded by the Research Council of Norway (grant
1028 number 228107) together with 10 academic and six industry (Equinor, Vår
1029 Energi, Aker BP, Lundin Energy Norway, OMV and Wintershall Dea) partners.
1030 Muhammad Hassaan was funded by the Suprabasins project (Research Council
1031 of Norway grant no. 295208). We thank to Schlumberger for providing us with
1032 academic licenses for Petrel software to do seismic interpretation. Two
1033 anonymous reviewers and the editors of this special volume provided comments,
1034 suggestions and advice that enhanced the clarity and scientific quality of the
1035 paper.

1036

1037

1038

1039

1040

1041

1042

1043

1044

1045 **References**

1046

1047 Allemand P. and Brun J.P.: Width of continental rifts and rheological layering of the
1048 lithosphere. *Tectonophysics*, 188, 63-69, 1991.

1049 Allmendinger,R.W.: : Inverse and forward numerical modeling of threeshear fault-
1050 propagation folds, *Tectonics*, 17(4), 640-656, 1998.

1051 Auzemery, A., E. Willingshofer, D. Sokoutis, J.P. Brun and Cloetingh S.A.P.L.,:
1052 Passive margin inversion controlled by stability of the mantle lithosphere,
1053 *Tectonophysics*, 817, 229042, 1-17, <https://doi.org/10.1016/j.tecto.2021.229042>,
1054 2021.

1055 Aydin,A. and Nur,A.:1982: Evolution of pull-apart basins and their scale
1056 independence. *Tectonics*, 1, 91-105, 1982.

1057

1058 Ballard J-F., Brun J-P and Van Ven Driessche J.: Propagation des chevauchements
1059 au-dessus des zones de décollement: modèles expérimentaux. *Comptes Rendus de*
1060 *l'Académie des Sciences, Paris*, 11, 305, 1249-1253, 1987.

1061

1062 Basile, C.: Transform continental margins – Part 1: Concepts and models.
1063 *Tectonophysics*, 661, pp.1-10. doi: 10.1016/j.tecto.2015.08.034, 2015.

1064

1065 Basile,C. and Brun,J.-P.: Transtensional faulting patterns ranging from pull-apart
1066 basins to transform continental margins: an experimental investigation, *Journal of*
1067 *Structural Geology*, 21,23-37, 1997.

1068

1069 Beauchamp,W., Barazangi,M., Demnati,A. and El Alji,M.: Intracontinental rifting
1070 and inversion: Missouri Basin and Atlas Mountains, Morocco. *American Association*
1071 *of Petroleum Geologists Bulletin*, 80(9), 1455-1482, 1996.

1072

1073 Bergh,S.G., Braathen,A. and Andresen,A.: Interaction of basement-involved and thin-
1074 skinned tectonism in the Tertiary fold-and-thrust belt of Central Spitsbergen,
1075 Svalbard. *American Association of Petroleum Geologists Bulletin*, 81(4), 637-
1076 661,1997.

1077

1078 Bergh,S.G. and Grogan,P.: Tertiary structure of the Sørkapp-Hornsund Region, South
1079 Spitsbergen, and implications for the offshore southern extension of the fold-thrust-
1080 belt. *Norwegian Journal of Geology*, 83, 43-60, 2003.

1081

1082 Biddle, K.T. and Christie-Blick, N., (eds.): *Strike-Slip Deformation, Basin*
1083 *Formation, and Sedimentation: Society of Economic Paleontologists and*
1084 *Mineralogists Special Publication*, 37, 386pp, 1985a.

1085

1086 Biddle, K.T. and Christie-Blick, N.: Glossary — Strike-slip deformation, basin
1087 formation, and sedimentation, *in*: Biddle, K.T., and Christie-Blick, N. (eds.): *Strike-*
1088 *Slip Deformation, Basin Formation, and Sedimentation: Society of Economic*
1089 *Paleontologists and Mineralogists Special Publication*, 37, 375-386, 1985b

1090

1091 Blaich,O.A., Tsikalas,F. and Faleide,J.I.: New insights into the tectono-stratigraphic
1092 evolution of the southern Stappen High and the transition to Bjørnøya Basin, SW

- 1093 Barents Sea, *Marine and Petroleum Geology*, 85, 89-105, doi:
 1094 10.1016/j.marpetgeo.2017.04.015, 2017.
 1095
- 1096 Breivik,A.J., Faleide,J.I. and Gudlaugsson,S.T.: Southwestern Barents Sea margin:
 1097 late Mesozoic sedimentary basins and crustal extension, *Tectonophysics*, 293, 21-44,
 1098 1998.
 1099
- 1100 Breivik,A.J., Mjelde,R., Grogan,P., Shinamura,H., Murai,Y. and Nishimura,Y.:
 1101 Crustal structure and transform margin development south of Svalbard based on
 1102 ocean bottom seismometer data. *Tectonophysics*, 369, 37-70 2003.
- 1103 Brekke, H.: The tectonic evolution of the Norwegian Sea continen- tal margin with
 1104 emphasis on the Vøring and Møre basins: Geological Society, London, Special
 1105 Publication, 136, 327–378, 2000.
- 1106 Brekke, H. and Riis, F.: Mesozoic tectonics and basin evolution of the Norwegian
 1107 Shelf between 60°N and 72°N. *Norsk Geologisk Tidsskrift*, 67, 295-322, 1987.
 1108
- 1109 Burchfiel, B.C. and Stewart,J.H.: "Pull-apart" origin of the central segment of Death
 1110 Valley, California. *Geological Society of America Bulletin*, 77, 439-442, 1966.
 1111
- 1112 Campbell,J.D.: *En échelon* folding, *Economical Geology*, 53(4), 448-472, 1958.
 1113
- 1114 Cartwright,J.A.: The kinematics of inversion in the Danish Central Graben. in:
 1115 M.A.Cooper & G.D.Williams (eds.): *Inversion Tectonics*. Geological Society of
 1116 London Special Publication, 44, 153-175, 1989.
 1117
- 1118 Casas, A.M., Gapals,D., Nalpas,T., Besnard,K. and Román-Berdiel,T.: Analogue
 1119 models of transpressive systems, *Jornal of Structural Geology*, 23,733-743, 2001
 1120
- 1121 Christie-Blick,N. and Biddle,K.T.: Deformation and basin formation along strike-slip
 1122 faults. *in*: Biddle,K.T. & Christie-Blick,N. (eds.): *Strike-slip deformation, basin*
 1123 *formation and sedimentation*. Society of Economic Mineralogists and
 1124 Palaeontologists (Tulsa Oklahoma), Special Publication, 37, 1-34, 1985.
 1125
- 1126 Cloos,H.: Experimenten zur inneren Tectonick, *Zentralblatt für Mineralogie,*
 1127 *Geologie und Palaentologie*, 1928B, 609-621, 1928.
 1128
- 1129 Cloos,H.: Experimental analysis of fracture patterns, *Geological Society of America*
 1130 *Bulletin*, 66(3), 241-256, 1955.
 1131
- 1132 Cooper,M. and Warren,M.J.: The geometric characteristics, genesis and petroleum
 1133 significance of inversion structures, in Law,R.D., Butler,R.W.H., Holdsworth,R.E.,
 1134 Krabbendam,M. & Strachan,R.A. (eds.): *Continental Tectonics and Mountain*
 1135 *Building: The Lagacy of Peache and Horne*, Geological Society of London, Special
 1136 Publication, 335, 827-846, 2010.
 1137
- 1138 Cooper,M.A., Williams,G.D., de Graciansky,P.C., Murphy,R.W., Needham,T., de
 1139 Paor,D., Stoneley,R., Todd,S.P., Turner,J.P. and Ziegler,P.A.: Inversion tectonics – a
 1140 discussion. Geological Society, London, Special Publications, 44, 335-347, 1989.

1141
1142 Coward, M.: Inversion tectonics, in: Hancock,P.L. (ed.): Continental Deformation,
1143 Pergamon Press, 289-304, 1994.
1144
1145 Coward, M.P., Gillcrist, R. and Trudgill, B.: Extensional structures and their tectonic
1146 inversion in the Western Alps, *in*: A.M.Roberts, G.Yielding & B.Freeman (eds.): The
1147 Geometry of Normal Faults. Geological Society of London Special Publication, 56,
1148 93-112 1991.
1149
1150 Crowell, J.C.: Displacement along the San Andreas Fault, California, Geological
1151 Society of America Special Papers, 71, 59pp, 1962.
1152
1153 Crowell, J.C.: Origin of late Cenozoic basins in southern California. in Dorr, R.H. and
1154 Shaver, R.H. (eds.): Modern and ancient geosynclinal sedimentation. SEPM Special
1155 Publication, 19, 292-303, 1974a
1156
1157 Crowell, J.C., 1974b: Implications of crustal stretching and shortening of coastal
1158 Ventura Basin, *in*: Howell,D.G. (ed.): Aspects of the geological history of the
1159 California continental Borderland, American Association of Petroleum Geologists,
1160 Pacific Section,Publication, 24, 365-382, 1974b
1161
1162 Cunningham, W.D. and Mann, P. (eds.): : Tectonics of Strike-Slip Restraining and
1163 Releasing Bends, Geological Society London Special Publication, 290, 482pp, 2007a.
1164
1165 Cunningham, W.D. and Mann, P.: Tectonics of Strike-Slip Restraining and Releasing
1166 Bends, *in*: Cunningham,W.D. & Mann,P. (eds.), 2007: Tectonics of Strike-Slip
1167 Restraining and Releasing Bends, Geological Society London Special Publication,
1168 290, 1-12, 2007b.
1169
1170 Dauteuil, O. and Mart, Y.: Analogue modeling of faulting pattern, ductile
1171 deformation, and vertical motion in strike-slip fault zones, *Tectonics*, 17(2), 303-310,
1172 1998.
1173
1174 Del Ventisette, C., Montanari, D., Sani, F., Bonini, M. and Corti, G.: Reply to
1175 comment by J. Wickham on “Basin inversion and fault reactivation in laboratory
1176 experiments”. *Journal of Structural Geology* 29, 1417–1418, 2007.
1177
1178 Dooley, T. and McClay, K.: Analog modeling of pull-apart basins, *American*
1179 *Association of Petroleum Geologists Bulletin*, 81(11), 1804-1826, 1997.
1180
1181 Dooley, T.P. and Schreurs, G.:Analogue modelling of intraplate strike-slip tectonics:
1182 A review and new experimental results, *Tectonophysics*, 574-575, 1-71, 2012
1183
1184 Doré, A.G. and Lundin, E.R.: Cenozoic compressional structures on the NE Atlantic
1185 margin: nature, origin and potential significance for hydrocarbon exploration.
1186 *Petroleum Geosciences*, 2, 299-311, 1996
1187
1188 Doré, A.G., Lundin, E.R., Gibbons, A., Sømme, T.O. and Tørudbakken, B.O.:
1189 Transform margins of the Arctic: a synthesis and re-evaluation *in*: Nemcok,M.,
1190 Rybár,S., Sinha,S.T., Hermeston,S.A. & Ledvényiová,L. (eds.): Transform Margins,:

1191 Development, Control and Petroleum Systems, Geological Society London, Special
1192 Publication, 431, 63-94, 2016.
1193
1194 Doré, A.G., Lundin, E.R., Jensen, L.N., Birkeland, Ø., Eliassen, P.E. and Fichler, C.:
1195 Principal tectonic events in the evolution of the northwest European Atlantic margin.
1196 In: A.J.Fleet & S.A.R.Boldy (eds.): Petroleum Geology of Northwest Europe:
1197 Proceedings of the Fifth Conference (Geological Society of London), 41-61, 1999.
1198
1199 Eidvin, T., Goll, R.M., Grogan, P., Smelror, M. and Ulleberg, K.: The Pleistocene to
1200 Middle Eocene stratigraphy and geological evolution of the western Barents Sea
1201 continental margin ta well site 731675-1 (Bjørnøya West area). Norsk Geologisk
1202 Tidsskrift, 78, 99-123 1988.
1203
1204 Eidvin, T., Jansen, E. and Riis,F.: Chronology of Tertiary fan deposits off the western
1205 Barents Sea: Implications for the uplift and erosion history of the Barents Shelf.
1206 Marine Geology, 112, 109-131, 1993.
1207
1208 Eldholm, O., Faleide, J.I. and Myhre, A.M.: Continent-ocean transition at the western
1209 Barents Sea/Svalbard continental margin. Geology, 15, 1118-1122, 1987.
1210
1211 Eldholm, O., Thiede, J., and Taylor, E.: Evolution of the Vøring volcanic margin, *in*:
1212 Eldholm, O., Thiede, J., and Taylor, E., (eds.): Proceedings of the Ocean Drilling
1213 Program, Scientific Results, 104: College Station (Ocean Drilling Program), TX,
1214 1033–1065, 1989.
1215
1216 Eldholm, O., Tsikalas, F. and Faleide,J.I.: Continental margin off Norway 62-
1217 75°N:Paleogene tectono-magmatic segmentation and sedimentation. Geological
1218 Society of London Special Publication, 197, 39-68, 2002
1219
1220 Emmons, R.C.: Strike-slip rupture patterns in sand models, Tectonophysics, 7, 71-87,
1221 1969.
1222
1223 Faugère, E., Brun, J.-P. and Van Den Driessche, J.: Bassins asymétriques en
1224 extension pure et en détachements:Modèles expérimentaux, Bulletin Centre
1225 Recherche Exploration et Production Elf Aquitaine, 10(2), 13-21, 1986.
1226
1227 Faleide, J.I., Bjørlykke, K. and Gabrielsen, R.H.: Geology of the Norwegian Shelf. *in*:
1228 Bjørlykke,K.: Petroleum Geoscience: From Sedimentary Environments to Rock
1229 Physics 2nd Edition, Springer-Verlag, Berlin Heidelberg, Chapter 25, 603 -637, 2015.
1230
1231 Faleide, J.I., Myhre, A.M. and Eldholm, O.: Early Tertiary volcanism at the western
1232 Barents Sea margin. in: A.C.Morton & L.M.Parsons (eds.): Early Tertiary volcanism
1233 and the opening of the NE Atlantic.Geological Society of London Special Publication,
1234 39,135-146, 1988.
1235
1236 Faleide, J.I., Tsikalas, F., Breivik, A.J, Mjelde, R., Ritzmann, O., Engen, Ø., Wilson,
1237 J. and Eldholm, O.: Structure and evolution of the continental margin off Norway and
1238 the Barents Sea. Episodes, 31(1), 82-91, 2008.
1239

- 1240 Faleide, J.I., Vågnes, E. and Gudlaugsson, S.T.: Late Mesozoic - Cenozoic evolution
1241 of the south-western Barents Sea in a regional rift-shear tectonic setting. *Marine and*
1242 *Petroleum Geology*, 10, 186-214, 1993
1243
- 1244 Fichler, C. and Pastore, Z.: Petrology and crystalline crust in the southwestern Barents
1245 Sea inferred from geophysical data. *Norwegian Journal of Geology*, 102, 41pp,
1246 <https://dx.doi.org/10.17850/njg102-2-2, 2022>.
1247
- 1248 Freund, R.: The Hope Fault, a strike-slip fault in New Zealand, *New Zealand*
1249 *Geological Survey Bulletin*, 86, 1-49, 1971.
1250
- 1251 Gabrielsen, R.H.: Structural elements in graben systems and their influence on
1252 hydrocarbon trap types. in: A.M. Spencer (ed.): *Habitat of Hydrocarbons on the*
1253 *Norwegian Continental Shelf*. *Norw. Petrol. Soc. (Graham & Trotman)*, 55 – 60,
1254 1986.
1255
- 1256 Gabrielsen, R.H., Færseth, R.B., Jensen, L.N., Kalheim, J.E. and Riis, F.: Structural
1257 elements of the Norwegian Continental Shelf. Part I: The Barents Sea Region.
1258 *Norwegian Petroleum Directorate, Bulletin*, 6, 33pp, 1990.
1259
- 1260 Gabrielsen, R.H., Grunnaleite, I. and Rasmussen, E.: Cretaceous and Tertiary
1261 inversion in the Bjørnøyrenna Fault Complex, south-western Barents Sea. *Marine and*
1262 *Petroleum Geology*, 142, 165-178, 1997.
1263
- 1264 Gac, S., Klitzke, P., Minakov, A., Faleide, J.I. and Scheck-Wenderoth, M.:
1265 Lithospheric strength and elastic thickness of the Barents Sea and Kara Sea region,
1266 *Tectonophysics*, 691, 120-132, doi: 10.106/j.tecto.2016.04.028, 2016.
1267
- 1268 Gaina, C., Gernigon, L. and Ball, P.: Palaeocene – Recent plate boundaries in the NE
1269 Atlantic and the formation of the Jan Mayen microcontinent. *Journal of the*
1270 *Geological Society, London*, 166(4), 601-616, 2009.
- 1271 Ganerød, M., Smethurst, M.A., Torsvik, T.H., Prestvik, T., Rouse, S., McKenna, C.,
1272 van Hinsbergen, D.J.J. and Hendriks, W.W.H.: The North Atlantic Igneous Province
1273 reconstructed and its relation to the Plume Generation Zone: the Antrim Lava Group
1274 revisited. *Geophysical Journal International*, 182, 183-202, doi: 10.1111/j.1365-
1275 246X.2010.04620.x, 2010.
- 1276 Giannenas, P.A.: The Structural Development of the Vestbakken Volcanic Province,
1277 Western Barents Sea. Relation between Faults and Folds, Unpublished Ms.Sci.thesis,
1278 University of Oslo, 89 pp., 2018
1279
- 1280 Gibson, G.M., Totterdell, J.M., White, N. Mitchell, C.H., Stacey, A.R., M. P. Morse,
1281 M.P. and A. Whitaker: Preexisting basement structures and its influence on
1282 continental rifting and fracture development along Australia's southern rifted margin,
1283 *Journal of the Geological Society of London*, 170, 365-377, 2013.
1284 .
1285
- 1286 Graymer, R.W., Langenheim, V.E., Simpson, R.W., Jachens, R.C. and Ponce, D.A.:
1287 Relative simple through-going fault planes at large-earthquake depth may be

1288 concealed by surface complexity of strike-slip faults, *in*: Cunningham,W.D. &
1289 Mann,P. (eds.): Tectonics of Strike-Slip Restraining and Releasing Bends, Geological
1290 Society London Special Publication, 290, 189-201, 2007.
1291
1292 Griera, A., Gomez Rivas, E. and Llorens,M.-G.: The influence of layer-interface
1293 geometry of single-layer folding. Geological Society of London Special Publication
1294 487, SP487:4, 2018.
1295
1296 Grogan, P., Østvedt-Ghazi, A.-M., Larssen, G.B., Fotland, B., Nyberg, K., Dahlgren,
1297 S. and Eidvin, T.: Structural elements and petroleum geology of the Norwegian sector
1298 of the northern Barents sea. *in*: Fleet,A.J. & Boldry,S.A.R. (eds.): Petroleum Geology
1299 of Northwest Europe: Proceedings of the 5th Conference, Geological Society of
1300 London, 247-259, 1999.
1301
1302 Groshong, R.H.: Half-graben structures: balanced models of extensional fault
1303 bend folds, Geological Society of America Bulletin, 101, 96-195, 1989
1304
1305 Gudlaugsson, S.T. and Faleide, J.I.: The continental margin between Spitsbergen &
1306 Bjørnøya, in: O.Eiken (ed.): Seismic Atlas of Western Svalbard, Norsk Polarinstitutt
1307 Meddelelser, 130, 11-13, 1994.
1308
1309 Gudlaugsson, S.T., Faleide, J.I., Johansen, S.E. and Breivik, A.J.: Late Palaeozoic
1310 structural development of the south-western Barents Sea. Marine and Petroleum
1311 Geology, 15, 73-102, 1998.
1312
1313 Hamblin, W.K.: Origin of "reverse drag" on the down-thrown side of normal
1314 faults, Geological Society of America Bulletin, 76, 1145-1164., 1965.
1315
1316 Hanisch, J.: The Cretaceous opening of the Northeast Atlantic. Tectonophysics, 101,
1317 1-23, 1984.
1318
1319 Harding, T.P.: Petroleum traps associated with wrench faults. American Association
1320 of Petroleum Geologists Bulletin, 58, 1290-1304, 1974.
1321
1322 Harding, T.P. and Lowell, J.D.: Structural styles, their plate tectonic habitats, and
1323 hydrocarbon traps in petroleum provinces, American Association of Petroleum
1324 Geologists Bulletin, 63,1016-1058, 1979.
1325
1326 Harland, W.B.: The tectonic evolution of the Arctic-North Atlantic Region, in:
1327 Taylor,J.H., Rutten,M.G., Hales,A.L., Shackelton,R.M., Nairn,A.E. & Harland:W.B.,:
1328 Discussion, A Symposium on Continental Drift, Philosophical Transactions of the
1329 Royal Society of London,, Series A, 258, 1088, 59-75, 1965.
1330
1331 Harland, W.B.: Contributions of Spitsbergen to understanding of tectonic evolution of
1332 North Atlantic Region, American Association of Petroleum Geologists, Memoir 12,
1333 817-851, 1969.
1334
1335 Harland, W.B.: Tectonic transpression in Caledonian Spitsbergen, Geological
1336 Magazine, 108, 27-42, 1971
1337

- 1338 Henk, A. and Nemcok, M.: Stress and fracture prediction in inverted half-graben
1339 structures. *Journal of Structural Geology*, 30(1), 81-97, 2008.
- 1340 Horni, J.Á., Hopper, J.R., Blischke, A., Geisler, W.H., Stewart, M., Mcdermott, K.,
1341 Judge, M., Erlendsson, Ö. and Ártng, U.E.: Regional Distribution of Volcanism
1342 within the North Atlantic Igneous Province. *The NE Atlantic Region: A Reappraisal*
1343 *of Crustal Structure, Tectonostratigraphy and Magmatic Evolution*. Geological
1344 Society, London, Special Publications, 447, 105–125,
1345 <https://doi.org/10.1144/SP447.18>, 2017.
- 1346 Horsfield, W.T., 1977: An experimental approach to basement-controlled
1347 faulting. *Geologie en Mijnbouw*, 56(4), 3634-370 1977.
- 1348
1349 Hubbert, M.K.: Theory of scale models as applied to the study of geologic
1350 structures, *Bulletin Geological Society of America*, 48, 1459-1520, 1937.
- 1351 Jebsen, C. and Faleide, J.I.: Tertiary rifting and magmatism at the western Barents
1352 Sea margin (Vestbakken volcanic province). III international conference on Arctic
1353 margins, ICAM III; abstracts; plenary lectures, talks and posters, 92, 1998.
- 1354 Khalil,S.M. and McClay,K.R.: 3D geometry and kinematic evolution of extensional
1355 fault-related folds, NW Red Sea, Egypt. in: Childs,C., Holdsworth,R.E.,
1356 Jackson,C.A.L., Manzocchi,T., Walsh,J.J & Yielding,G. (eds.): *The Geometry and*
1357 *Growth of Normal Faults*, Geological Society, London, Special Publication 439,
1358 doi.org/10.1144/SP439.11, 2016.
- 1359
1360 Klinkmüller, M., Schreurs, G., Rosenau, M. and Kemnitz, H.: Properties of
1361 granular analogue model materials: a community wide survey. *Tectonophysics*
1362 684, 23–38. <http://dx.doi.org/10.1016/j.tecto.2016.01.017>, 2016.
- 1363
1364 Knutsen, S.-M. and Larsen,K.I.: The late Mesozoic and Cenozoic evolution of the
1365 Sørvestsnaget Basin: A tectonostratigraphic mirror for regional events along the
1366 Southwestern Barents Sea Margin? *Marine and Petroleum Geology*, 14(1), 27-54,
1367 1997.
- 1368
1369 Kristensen, T.B., Rotevatn, A., Marvik, M., Henstra, G.A., Gawthorpe, R.L. and
1370 Ravnås, R.: Structural evolution of sheared basin margins: the role of strain
1371 partitioning. *Sørvestsnaget Basin, Norwegian Barents Sea, Basin Research*, (2017), 1-
1372 23, doi:10.1111/bre.12235, 2017.
- 1373
1374 Le Calvez, J-H. and Vendeville, : Experimental designs to mode along strike-slip fault
1375 interaction. *in*: Scellart, W.P. & Passcheir, C. (eds.). *Analogue Modeling of large-*
1376 *scale Tectonic Processes*, *Journal of Virtual Explorer*, 7, 7-23, 2002.
- 1377
1378 Leever, K.A., Gabrielsen, R.H., Sokoutis, D. and Willingshofer, E.: The effect of
1379 convergence angle on the kinematic evolution of strain partitioning in transpressional
1380 brittle wedges: insight from analog modeling and high resolution digital image
1381 analysis. *Tectonics*, 30, TC2013, 1-25, doi: 10.1029/2009TC002649, 2011a.
- 1382

- 1383 Leever, K.A., Gabrielsen, R.H., Faleide, J.I. and Braathen, A.: A transpressional
1384 origin for the West Spitsbergen Fold and Thrust Belt - insight from analog modeling.
1385 Tectonics, 30, TC2014, 1- 24, doi: 10.1029/2010TC002753, 2011b.
1386
- 1387 Libak, A., Mjelde, R., Keers, H., Faleide, J.I. and Murai, Y.: An integrated
1388 geophysical study of Vestbakken Volcanic Province, western Barents Sea continental
1389 margin, and adjacent oceanic crust, Marine Geophysical Research, 33(2), 187-207,
1390 2012.
1391
- 1392 Lorenzo, J.M.: Sheared continental margins: an overview, Geo-Marine Letters, 17(1),
1393 1-3, 1997
- 1394 Lowell, J.D., 1972: Spitsbergen Tertiary orogenic belt and the Spitsbergen fracture
1395 zone, Geol. Soc. Am. Bull., 83, 3091–3102, doi:10.1130/0016-
1396 7606(1972)83[3091:STOBAT]2.0.CO;2, 1972.
- 1397 Lundin, E.R. and Doré, A.G.: A tectonic model for the Norwegian passive margin
1398 with implications for the NE Atlantic.: Early Cretaceous to break-up. Journal of the
1399 Geological Society London, 154, 545-550, 1997.
1400
- 1401 Lundin, E.R., Doré, A.G., Rønning, K. and Kyrkjebø, R.: Repeated inversion in the
1402 Late Cretaceous-Cenozoic northern Vøring Basin, offshore Norway, Petroleum
1403 Geoscience, 19(4), 329-341, 2013.
1404
- 1405 Luth, S., Willingshofer, E., Sokoutis, D. and Cloetingh, S.: analogue modelling of
1406 continental collision: Influence of plate coupling on mantle lithosphere subduction,
1407 crustal deformation and surface topography, Tectonophysics, 4184, 87-102, doi:
1408 10.1016/j.tecto2009.08.043, 2010.
- 1409 Maher, H. D., Jr., Bergh, S., Braathen, A. and Ohta, Y.: Svartfjella, Eidembukta, and
1410 Daudmannsodden lineament: Tertiary orogen-parallel motion in the crystalline
1411 hinterland of Spitsbergen's fold-thrust belt, Tectonics, 16(1), 88–106,
1412 doi:10.1029/96TC02616, 1997.
- 1413 Mandl, G., de Jong, L.N.J. and Maltha, A.: Shear zones in granular material. Rock
1414 Mechanics, 9, 95–144, 1977.
1415
- 1416 Manduit, T. and Dauteuil, O.: Small scale modeling of oceanic transform zones,
1417 Journal of Geophysical Research, 101(B9), 20195-20209, 1996.
1418
- 1419 Mann, P.: Global catalogue, classification and tectonic origins of restraining and
1420 releasing bends on active and ancient strike-slip fault systems. *in*: Cunningham, W.D.
1421 and Mann, P. (eds.), 2007: Tectonics of Strike-Slip Restraining and Releasing Bends,
1422 Geological Society London Special Publication, 290, 13-142, 2007.
1423
- 1424 Mann, P., Hempton, M.R., Bradley, D.C. and Burke, K.: Development of pull-apart
1425 basins. Journal of Geology, 91(5), 529-554, 1983.
1426
- 1427 Mascle, J. & Blarez, E.: Evidence for transform margin evolution from the Ivory
1428 Coast Ghana continental margin, Nature, 326, 378-381, 1987.

1429
1430 McClay, K.R., 1990: Extensional fault systems in sedimentary basins. A review of
1431 analogue model studies, *Marine and Petroleum Geology*, 7, 206-233, 1990.
1432
1433 Mitra, S.: Geometry and kinematic evolution of inversion structures. *American*
1434 *Association of Petroleum Geologists Bulletin*, 77, 1159-1191, 1993.
1435
1436 Mitra, S. and Paul, D.: Structural geology and evolution of releasing and
1437 constraining bends: Insights from laser-scanned experimental models, *American*
1438 *Association of Petroleum Geologists Bulletin*, 95(7), 1147-1180, 2011.
1439
1440 Morgenstern, N.R. and Tchalenko, J.S.: Microscopic structures in kaolin subjected to
1441 direct shear, *Géotechnique*, 17, 309-328, 1967.
1442
1443 Mosar, J., Torsvik, T.H. & the BAT Team: Opening of the Norwegian and Greenland
1444 Seas: Plate tectonics in mid Norway since the late Permian. in: E.Eide (ed.):
1445 BATLAS. Mid Norwegian plate reconstruction atlas with global and Atlantic
1446 perspectives. Geological Survey of Norway, 48-59, 2002.
1447
1448 Mouslopoulou, V., Nicol, A., Little, T.A. and Walsh, J.J.: Terminations of large-
1449 strike-slip faults: an alternative model from New Zealand, in: Cunningham, W.D. and
1450 Mann, P. (eds.): *Tectonics of Strike-Slip Restraining and Releasing Bends*,
1451 *Geological Society London Special Publication*, 290, 387- 415, 2007.
1452
1453 Mouslopoulou, V., Nicol, A., Walsh, J.J., Beetham, D. and Stagpoole, V.: Quaternary
1454 temporal stability of a regional strike-slip and rift fault interaction. *Journal of*
1455 *Structural Geology*, 30, 451-463, 2008.
1456
1457 Myhre, A.M. and Eldholm, O.: The western Svalbard margin (74-80°N). *Marine and*
1458 *Petroleum Geology*, 5, 134-156, 1988.
1459
1460 Myhre, A.M., Eldholm, O. and Sundvor, E.: The margin between Senja and
1461 Spitsbergen Fracture Zones: Implications from plate tectonics. *Tectonophysics*, 89,
1462 33-50, 1982.
1463
1464 Naylor, M.A., Mandl, G and Sijpestijn, C.H.K.: Fault geometries in basement-induced
1465 wrench faulting under different initial stress states. *Journal of Structural Geology*, 8,
1466 737-752, 1986.
1467
1468 Nemcok, M., Rybár, S., Sinha, S.T., Hermeston, S.A. and Ledvényiová, L.:
1469 Transform margins: development, controls and petroleum systems – an introduction.
1470 in: Nemcok, M., Rybár, S., Sinha, S.T., Hermeston, S.A. and Ledvényiová, L. (eds.):
1471 *Transform Margins: Development, Control and Petroleum Systems*, Geological
1472 Society London, Special Publication, 431, 1-38, 2016.
1473
1474 Odonne, F. and Vialon, P.: Analogue models of folds above a wrench fault,
1475 *Tectonophysics*, 99,31-46, 1983
1476

1477 Pace, P. and Calamita, F.: Push-up inversion structures v. fault-bend reactivation
1478 anticlines along oblique thrust ramps: examples from the Apennines fold-and-thrust-
1479 belt, Italy, *Journal Geological Society London*, 171, 227-238, 2014.
1480
1481 Pascal, C. and Gabrielsen, R.H.: Numerical modelling of Cenozoic stress patterns in
1482 the mid Norwegian Margin and the northern North Sea. *Tectonics*, 20(4), 585-599,
1483 2001.
1484
1485 Pascal, C., Roberts, D. and Gabrielsen, R.H.: Quantification of neotectonic stress
1486 orientations and magnitudes from field observations in Finnmark, northern Norway.
1487 *Journal of Structural Geology*, 27, 859-870, 2005.
1488
1489 Peacock, D.C.P., Nixon, C.W., Rotevatn, A., Sanderson, D.J. and Zuluaga, L.F.:
1490 Glossary of fault and other fracture networks, *Journal of Structural Geology*, 92,
1491 12-29, doi: 10.1016/j.jgs2016.09.008, 2016.
1492
1493 Perez-Garcia, C., Safranova, P.A., Mienert, J., Berndt, C. and Andreassen, K.:
1494 Extensional rise and fall of a salt diapir in the Sørvestsnaget Basin, SW Barents Sea.
1495 *Marine and Petroleum Geology*, 46, 129-134, 2013.
1496
1497 Planke, S., Alvestad, E. and Eldholm, O.: Seismic characteristics of
1498 basaltic extrusive and intrusive rocks: The Leading Edge, 18(3), 342-348. [https://doi-
1499 org.ezproxy.uio.no/10.1190/1.1438289](https://doi-org.ezproxy.uio.no/10.1190/1.1438289), 1999.
1500
1501 Ramberg, H.: Gravity, deformation and the Earth's crust, Academic Press, New York,
1502 214pp, 1967.
1503
1504 Ramberg, H.: Gravity, deformation and the Earth's crust, 2nd edition. Academic
1505 Press, New York 452pp, 1981
1506
1507 Ramsay, J.G. and Huber, M.I., 1987: The techniques of modern structural geology.
1508 Vol. 2: Folds and fractures. Academic Press, London, 309-700, 1987.
1509
1510 Reemst, P., Cloetingh, S. and Fanavoll, S.: Tectonostratigraphic modelling of
1511 Cenozoic uplift and erosion in the south-western Barents Sea. *Marine and Petroleum
1512 Geology*, 11, 478-490, 1994.
1513
1514 Richard, P.D., Ballard, B., Colletta, B and Cobbold, P.R.: Naissance et evolution de
1515 failles au dessus d'un décrochement de socle: Modélisation experimental et
1516 tomographie, *C. R. Acad.Sci. Paris*, 308,9, 2111-2118, 1989.
1517
1518 Richard, P.D. and Cobbold, P.R.: Structures et fleur positives et décrochements
1519 crustaux: mdélisation analogique et interpretation mecanique, *C.R.Acad.Sci.Paris*,
1520 308, 553-560, 1989.
1521
1522 Richard, P. and Krantz, R.W.: Experiments on fault reactivation in strike-slip mode,
1523 *Tectonophysics*, 188, 117-131, 1991.
1524

- 1525 Richard, P., Mocquet, B. and Cobbold, P.R., 1991: Experiments on simultaneous
1526 faulting and folding above a basement wrench fault, *Tectonophysics*, 188, 133-141.
1527 1991.
- 1528
- 1529 Riedel, W.: Zur Mechanik geologischer Brucherscheinungen. *Centralblatt für*
1530 *Mineralogie, Geologie und Paläontologie*, 1929B, 354-368, 1929.
- 1531
- 1532 Riis, F., Vollset, J. & Sand, M.: Tectonic development of the western margin of the
1533 Barents Sea and adjacent areas. in: M.T. Halbouty (ed.): *Future petroleum provinces*
1534 *of the World. American Association of Petroleum Geologists Memoir*, 40, 661-667,
1535 1986.
- 1536
- 1537 Roberts, D.G., : Basin inversion in and around the British Isles, in: M.A. Cooper &
1538 G.D. Williams (eds.): *Inversion Tectonics. Geological Society of London Special*
1539 *Publication*, 44, 131-150, 1989.
- 1540
- 1541 Ryseth, A., Augustson, J.H., Charnock, M., Haugsrud, O., Knutsen, S.-M., Midbøe,
1542 P.S., Opsal, J.G. and Sundsbø, G.: Cenozoic stratigraphy and evolution of the
1543 Sørvestsnaget Basin, southwestern Barents Sea. *Norwegian Journal of Geology*, 83,
1544 107-130, 2003.
- 1545
- 1546 Saunders, A.D., Fitton, J.G., Kerr, A.C., Norry, M.J., and Kent, R.W.: The North
1547 Atlantic Igneous Province: *Geophysical Monograph* 100, American Geophysical
Union, 45–93, 1997.
- 1548
- 1549 Scheurs, G.: Experiments on strike-slip faulting and block rotation, *Geology*, 22, 567-
1550 570, 1990.
- 1551
- 1552 Schreurs, G.: Fault development and interaction in distributed strike-slip shear zones:
1553 an experimental approach. in: Storti, F., Holdsworth, R.E. and Salvini, F. (eds):
1554 *Intraplate Strike-slip Deformation Belts, Geological Society of London Special*
1555 *Publication*, 210, 35-82., 2003.
- 1556
- 1557 Schreurs, G., and Colletta, B.. Analogue modelling of faulting in zones of
1558 continental transpression and transtension. in: Holdsworth, R.E., Strachan, R.A.,
1559 Dewey, J.F. (eds.), *Continental Transpressional and Transtensional Tectonics*,
1560 *Geological Society of London Special Publication*, London, 135, 59–79, 1998.
- 1561
- 1562 Schreurs, G. and Colletta, B.: Analogue modelling of continental transpression
1563 and transtension. in: Scellart, W.P. & Passchier, C. (eds.): *Analogue Modelling of*
1564 *Large-scale Tectonic Processes. Journal of the Virtual Explorer*, 7, 103-114,
1565 2003.
- 1566
- 1567 Seiler, C., Fletcher, J.M., Quigley, M.C., Gleadow, A.J and Kohn, B.P.: Neogene
1568 structural evolution of the Sierra San Felipe, Baja California: evidence of proto-gulf
1569 transtension in the Gulf Extensional Province? *Tectonophysics*, 488(1), 87-109, 2010.
- 1570
- 1571 Sibuet, J.C. and Mascle, J.: Plate kinematic implications of Atlantic equatorial
1572 fracture zone trends. *Journal of Geophysical Research*, 85, 3401-3421, 1978.
- 1573
- 1574 Sims, D., Ferrill, D.A. and Stamatakos, J.A.: Role of a brittle décollement in the

- 1573 development of pull-apart basins: experimental results and natural examples. Journal
1574 of Structural Geology, 21, 533-554, 1999.
- 1575
- 1576 Sokoutis D.: Finite strain effects in experimental mullions. Journal of Structural
1577 Geology, 9, 233-249, 1987.
- 1578 Stearns, D.W., 1978: Faulting and forced folding in the Rocky Mountains
1579 Foreland, Geological Society of America Memoir, 151, 1-38, 1978
- 1580
- 1581 Sylvester, A.G. (ed); 1985: Wrench Fault Tectonics, Selected papers reprinted from
1582 the AAPG Bulletin and other geological journals, American Association of Petroleum
1583 Geologists Reprint Series 28,3 74pp, 1985.
- 1584
- 1585 Sylvester, A.G.: Strike-slip faults. Geological Society of America Bulletin, 100, 1666-
1586 1703, 1988.
- 1587
- 1588 Taylor,B., Goodlife,A. and Martinez,F.: Initiation of transform faults at rifted
1589 continental margins, Comtes Rendu Geosciences, 341, 428-438, 2009.
- 1590
- 1591 Talwani, M. & Eldholm, O.: Evolution of the Norwegian-Greenland Sea. Geological
1592 Society of America Bulletin, 88, 969-999, 1977.
- 1593
- 1594 Tchalenko, J.S: Similarities between shear zones of different magnitudes. Geological
1595 Society of America Bulletin, 81, 1625-1640,1970
- 1596
- 1597 Tron, V. and Brun J-P.: Experiments on oblique rifting in brittle-ductile systems.
Tectonophysics, 188(1/2), 71-84, 1991.
- 1598
- 1599 Twiss, R.J. and Moores, E.M.: Structural Geology, 2nd Edition, W.H.Freeman & Co.,
New York, 736pp, 2007.
- 1600
- 1601 Ueta, K., Tani ,K. and Kato,T.: Computerized X-ray tomography analysis of three-
1602 dimensional fault geometries in basement-induced wrench faulting, Engineering
1603 Geology, 56, 197-210, 2000
- 1604
- 1605 Uliana, M.A., Arteaga, M.E., Legarreta, L., Cerdan, J.J. and Peroni, G.O.: Inversion
1606 structures and hydrocarbon occurrence in Argentina. *in*: Buchanan,J.G. &
1607 Buchanan,P.G. (eds.): Basin Inversion, Geological Society London Special
1608 Publication, 88, 211-233, 1995
- 1609
- 1610 Vågnes,E.,1997: Uplift at thermo-mechanically coupled ocean-continent transforms:
1611 modeled at the Senja Fracture Zone, southwestern Barents Sea. Geo-Marine Letters,
1612 17, 100-109, 1997.
- 1613
- 1614 Vågnes, E., Gabrielsen, R.H. and Haremo. P.: Late Cretaceous-Cenozoic intraplate
1615 contractional deformation at the Norwegian continental shelf: timing, magnitude and
regional implications. Tectonophysics, 300, 29-46, 1998.
- 1616
- 1617 Weijermars, R. and Schmeling, H.: Scaling of Newtonian and non-Newtonian
fluid dynamics without inertia for quantitative modelling of rock flow due to

1618 gravity (including the concept of rheological similarity. *Physics of the Earth and*
1619 *Planetary Interiors*, 43, 316–330, 1986.

1620 Wilcox, R.E., Harding, T.P. and Selby, D.R.: Basic wrench tectonics. *American*
1621 *Association of Petroleum Geologists Bulletin*, 57, 74–69, 1973

1622

1623 Williams, G.D., Powell, C.M., and Cooper, M.A.: Geometry and kinematics of
1624 inversion tectonics. in: M.A.Cooper & G.D.Williams (eds.): *Inversion Tectonics*.
1625 *Geological Society of London Special Publication*, 44, 3–16, 1989.

1626

1627 Willingshofer, E., Sokoutis, D. and Burg, J.-P.: Lithosphere-scale analogue modelling of
1628 collision zones with a pre-existing weak zone, *in*: Gapais, D., Brun, J.P. & Cobbold, P.R.
1629 (eds.): *Deformation Mechanisms, Rheology and Tectonics: from Minerals to the*
1630 *Lithosphere*, *Geological Society London Special Publication*, 43, 277–294, 2005.

1631

1632 Willingshofer, E., Sokoutis, D., Beekman, F., Schönebeck, F., Warsitzka, J.-M., Michael,
1633 M. and Rosenau, M.: Ring shear test data of feldspar sand and quartz sand used in
1634 the Tectonic Laboratory (TeLab) at Utrecht University for experimental Earth
1635 Science applications. V. 1. GFZ Data Service.
1636 <https://doi.org/10.5880/idgeo.2018.072>, 2018.

1637

1638 Woodcock, N.H. and Fisher, M., 1986: Strike-slip duplexes. *Journal of Structural*
1639 *Geology*, 8(7), 725–735, 1986.

1640

1641 Woodcock, N.H. and Schubert, C.: Continental strike-slip tectonics. in: P.L.Hancock
1642 (ed.): *Continental Deformation* (Pergamon Press), 251–263, 1994.

1643

1644 Yamada, Y. and McClay, K.R.: Analog modeling of inversion thrust structures,
1645 experiments of 3D inversion structures above listric fault systems, in: McClay, K.R.
1646 (ed.): *Thrust Tectonics and Petroleum Systems*, *American Association of Petroleum*
1647 *Geologists Memoir*, 82, 276–302, 2004.

1648

1649

1650

1651

1652

1653

1654

1655

1656

1657

1658

1659

1660